3rd International Workshop on Polymer/Metal Nanocomposites

Nanoworkshop 2007 in Kobe

October 3-5, 2007

Abstracts

Graduate School of Engineering

Kobe University

Organizing committee

Shigehito Deki (Chair, Kobe University, Japan)
Kensuke Akamatsu (Konan University, Japan)
H. Biederman (Charles University Prague, Czech Republic)
Walter Caseri (ETH Zürich, Switzerland)
Franz Faupel (Christian Albrecht University of Kiel, Germany)
Detlev Fritsch(GKSS, Research Centre, Germany)
Kei Murakoshi (Hokkaido University, Japan)
Takashi Nishino (Kobe University, Japan)
Wataru Sugimoto (Shinshu University, Japan)
Tsukasa Torimoto (Nagoya University, Japan)

Secretariat General

Minoru Mizuhata (Kobe University, Japan)

Published on September 28, 2007
Graduate School of Engineering, Kobe University
1-1 Rokkodai-cho, Nada, Kobe 657-8501, Japan

Welcome to Nanoworkshop 2007 in KOBE!

International Workshop on Polymer/Metal Nanocomposites; "Nanoworkshop" has begun in 2003 at University of Kiel. The 3rd workshop will be held in Kobe University located at the Kansai Area of Japan. Polymer/ Metal nanocomposites are focused in the viewpoints such as;

-PVD and CVD based preparation techniques
-Preparation by wet chemical methods
-Novel preparation approaches
-Optical properties and applications
-Magnetic properties
-High-density data storage
-Magnetic devices for GHz
-Catalytic properties and reactive membranes
-Electronic properties and devices
-Biological and medial applications
-Self-assembled polymer/metal composites

The meeting place is Kobe University Centennial Hall (Shindai Hall) (Kobe, JAPAN) at the foot of the Mt. Rokko in Kobe. Kobe city is located in the Kansai region of Japan to the west of Osaka. Kobe is a part of the Osaka-Kobe-Kyoto metropolitan sprawl. A great many things account for Kobe's unique charm – the beauty of the surrounding sea and mountains, the international cuisine, the delicious sweets, the exotic and fashionable ambience, and the historic houses and Important Cultural Assets, along with a variety of other delights.

The Nanoworkshop 2007 aims to bring together physicists, chemists, and engineers from academics and industry in a productive, manageable ambience. The scope of the workshop ranges from advanced preparation techniques to resulting new properties and industrial applications. Theoretical work and computer simulations are also included. The nanocomposites may consist of polymer/metal in the shape of nanoclusters, nanotubes, nanofibers, and nanowires. Contributions discussing functional properties of polymer/carbon composites are also welcome. Sufficient time to get acquainted among each other will be allocated after the talks for discussion and in the poster session. The programme will consist of Plenary Lecture, Invited Lectures, Oral presentations (20 min) and posters.

We hope the participants enjoy each other throughout Nanoworkshop 2007.

Chair
Shigehito Deki, Prof.
Department of Chemical Science & Engineering
Faculty of Engineering, Kobe University

Time Table

Oct.3	**Takigawa Kinen Gakujutsu Koryu Kaikan**	
15:00-	**Registration**	
17:00-	**Get Together Meeting**	

Oral Presentation (Oct. 4-Oct. 5 Rokko Hall)

Oct. 4 Session - Kobe University Centennial Hall (Shindai Hall)

Chairman – Prof. Shigehito Deki

9:00-	Opening Remarks	
PL-1 9:10-9:40	[Plenary Lecture] “Polymer-based nanocomposites for functional applications” Franz Faupel, Vladimir Zaporojtchenko, Henry Greve, Ulrich Schurmann, Haile Takele, Christian Pochstein, Venkata Sai Kiran Chakravadhanula, Amit Kulkarni, A. Gerber, Eckhard Quandt, and Rainer Podschun (University of Kiel, Germany)	3
IL-2 9:40-10:05	[Invited Lecture] “Metal Nanoclusters in Polymers of High Free Volume” Detlev Fritsch (GKSS-Forschungszentrum, Germany)	5
IL-3 10:05-10:30	[Invited Lecture] “Introduction of Inorganic Components into Polymer Using Iodine” Yasuo Gotoh, Akio Kawaguchi, Yoshie Fujimori, Yutaka Ohkoshi, and Masanobu Nagura (Shinshu University and Kyoto University, Japan)	6
IL-4 10:30-10:55	[Invited Lecture] “Pt Modified with RuO_2 Nanosheets as Improved Fuel Cell Electrocatalysts” Wataru Sugimoto, Takahiro Saida, and Yoshio Takasu (Shinshu University, Japan)	7

Chairman – Prof. Dr. Franz Faupel

IL-5 10:55-11:20	[Invited Lecture] “Chemical Route to Synthesize Metal/Polymer Nanocomposites with Controlled Microstructures” Kensuke Akamatsu (Konan University and PRESTO-JST, Japan)	10

OP-6
11:20-11:40 "Photoinduced Hydrogen Production with Carotenoid-chlorophyll-platinum Nano-conjugated Micellar System" 11
Yutaka Amao and Yoshiko Fuchino (Oita University, Japan)

OP-7
11:40-12:00 "Synthesis of palladium-LDPE nanocomposites by implantation of neutral clusters produced by a supersonic cluster source" 13
Luca Ravagnan, Sara Rebasti, Giorgio Divitini, Valeria Cassina, Paolo Piseri, Paolo Milani (University of Milano, Italy)

Lunch

Chairman – Dr. Yasuo Gotoh

OP-8
13:30-13:50 Investigation of sol-gel templated polymer nanocomposite films for photovoltaic applications 15
Jan Perlich, Mine Memesa, Ya-Jun Cheng, Jochen S. Gutmann, Peter Mueller-Buschbaum (Technische Universität München, Max-Planck Institute for Polymer Research, and University of Mainz, Germany)

IL-9
13:50-14:15 [Invited Lecture]
"Structure and morphology of nanostructured noble metal-polymer bilayers for optical applications" 17
Stephan V. Roth, Rainer Gehrke, Georg Jakopic, Ralf Rohlsberger, Harald Walter, Ralph Domnick, Mottakin Abul-Kashem, and Peter Muller-Buschbaum (DESY, Joanneum Research, CSEM SA, Ara-Coatings GmbH & Co. KG, TU Munchen, Germany)

IL-10
14:15-14:40 [Invited Lecture]
"Physicochemical Properties and Applications of Polymer-Metal Nanocomposite Films near the Percolation Threshold" 19
Vladimir Zaporojtchenko, H. Takele, H. Greve, C. Hanisch, L. Li, V.S.K. Chakravadhanula, A.Kulkarni, T. Strunskus and F. Faupel (University of Kiel, Germany)

Chairman – Dr. Kensuke Akamatsu

IL-11
14:40-15:05 [Invited Lecture]
"Magnetic and structural properties of thin polymer films with embedded super-paramagnetic γ-Fe_2O_3 nano-particles" 20
Peter Müller-Buschbaum, Mottakin M. Abul Kashem, Jan Perlich, Leander Schulz (Technische Universität München, Germany and Universite de Fribourg, Switzerland)

Coffee Break

IL-12
15:30-15:55 [Invited Lecture]
"Characteristics of Scattering Photons from a Small Number of Molecules at Metal Nanogap" 21
Kei Murakoshi, Yoshitaka Sawai, Mai Takase, and Hideki Nabika (Hokkaido University, Japan)

IL-13
15:55-16:20 [Invited Lecture]
"Clean Synthesis of Highly Dispersed Metal Nanoparticles in Ionic Liquids Using a Sputter Deposition Technique" 23
Tsukasa Torimoto, Ken-ichi Okazaki, Tomonori Kiyama, Kaori Hirahara, Nobuo Tanaka, and Susumu Kuwabata (Nagoya University and Osaka University, Japan)

16:30-17:30 Poster Session (Kobe University Centennial Hall)

17:30-19:30 Banquet

Oct. 5 Session - Kobe University Centennial Hall (Shindai Hall)

Chairman – Prof. Dr. Detlev Fritsch

CL-14
9:10-9:40 [Chairs Lecture]
Novel Fabrication Process of Polymer/ Metal Nanoparticle Composite for Electrode materials 25
Shigehito Deki and Minoru Mizuhata (Kobe University, Japan)

OP-15
10:00-10:20 "In-situ observation of metal nanoparticle ordering at the air-water-substrate boundary in colloidal solutions" 27
Stephan V. Roth, Tina Autenrieth, Gerhard Grubel, Manfred Burghammer, and Christian Riekel (DESY, Germany and ESRF,France)

OP-16
10:20-10:45 [Invited Lecture]
"Properties of metal nanowires on polymers" 29
Rainer Adelung (University of Kiel, Germany)

Chairman – Prof. Dr. Rainer Adelung

OP-17
11:00-11:25 [Invited Lecture] 30
"Eco- & Nano-Polymer Composites"
Takashi Nishino, Masaru Kotera, Yukari Sakagami, Aya Nakai, and Yoshimasa Urushihara (Kober University and Hyogo Science and Technology, Japan)

OP-18
11:25-11:55 "Real-time spectroscopic ellipsometry of silver nanoparticle formation in polymer thin films" 32
Thomas W.H. Oates (Sydney University, Australia)

11:55- Closing Address

Poster Session (10/4 16:30-17:30) 35

Organizer – Dr. Minoru Mizuhata

PS-1
"Titanyl Phthalocyanine and/or Plasma Polymerized Thiophene and Titania Bilayer Thin Films" 37
Martin Drabik, Adam M. Zachary, Y. Choi, Jan Hanus, J. Matousek, Oleksandr Polonskyi, Jiri Tousek, Jana Touskova, Vera Cimrova, Zdenek Remes, Danka Slavinska, Hynek Biederman, and Luke Hanley (Charles University in Prague, Czech, University of Illinois at Chicago, USA, and Academy of Sciences of the Czech Republic, Czech)

PS-2
"Ni Nanoparticles/DVB Microsphere Composite : Control of Particle Diameter and Interparticle Spacing" 39
Takaaki Tsuruoka, Satoshi Adachi, Shingo Ikeda, Kensuke Akamatsu, Hidemi Nawafune, and Satoshi Tomita (Konan University, PREST-JST, and Nara Institute of Science and Technology, Japan)

PS-3
"Three-dimensional Optical Arrangements of Magnetic Semiconductor EuS Nanoaggregations" 40
Atsushi Tanaka, Tadao Sugiura, Yasuchika Hasegawa, and Tsuyoshi Kawai
(Nara Institute of Science and Technology, Japan)

PS-4
"Molecularly Imprinted Polymer Nanocomposite for Highly Sensitive Surface Plasmon Resonance (SPR) Detection of Herbicides" 42
Megumi Takayose, Jun Matsui, Kensuke Akamatsu, Hidemi Nawafune, Katsuyuki Tamaki, and Naoki Sugimoto (Konan University, Japan)

PS-5
"Synthesis and spectroscopic studies of dendrimer-Au hybrid nanoclusters" 44
Yoshiaki Murase, Takanobu Kitagawa, Akinori Tanaka, Hidehiro Yasuda, Yuichi Negishi, and Tatsuya Tsukuda (Kobe University and Institute for Molecular Science, Japan)

PS-6
"Molecular Manipulation at Small Metallic Gate" 46
Hideki Nabika, Baku Takimoto, Masahiro Oowada, Naozumi Iijima, Kei Murakoshi
(Hokkaido University, Japan)

Exhibitions

Rigaku

NBC The most advanced mesh technology in the world

Supporting organizations

AsahiKASEI 旭化成株式会社

BANDO BANDO CHEMICAL INDUSTRIES, LTD.

kuraray

MITSUBOSHI MITSUBOSHI BELTING LTD.

MORESCO 株式会社 松村石油研究所

SRI Hybrid Limited (SRI Hybrid Ltd.)

SUMITOMO BAKELITE CO., LTD.

KOBE UNIVERSITY Nano-engineering Research, OAST, Kobe University

Deutsche Forschungsgemeinschaft DFG

Oral Presentations (OP)

Including

Plenary Lecture

Chairs Lecture

Invited Lectures (IL)

Plenary Lecture -1

Polymer-based nanocomposites for functional applications

Franz Faupel[1*],Vladimir Zaporojtchenko[1], Henry Greve[1],
Ulrich Schürmann[1], Haile Takele[1], Christian Pochstein[1],
Venkata Sai Kiran Chakravadhanula[1], Amit Kulkarni[1],
A. Gerber[2], Eckhard Quandt[2], and Rainer Podschun[3]
[1]Christian-Albrechts-Universität zu Kiel,
Lehrstuhl für Materialverbunde, Kaiserstr. 2,
D-24143 Kiel, Germany.
[2] Christian-Albrechts-Universität zu Kiel, Lehrstuhl für Anorganische Funktionsmaterialien,
Kaiserstr. 2, D-24143 Kiel, Germany.
[3]Christian-Albrechts-Universität zu Kiel, Institut für Infektionsmedizin, Universitätsklinikum
Schleswig-Holstein, Campus Kiel, Brunswiker Str. 4, 24105 Kiel, Germany

Hybrid materials consisting of metal nanoparticles dispersed in a dielectric matrix are the subject of extensive research due to their novel functional properties offering hosts of new applications. Polymers are particularly attractive as matrix. Consequently, various approaches have been reported to incorporate metal nanoparticles into polymers. The present talk is concerned with the preparation of polymer-based nanocomposites by vapor phase co- and tandem deposition and the resulting functional properties. The techniques involve evaporation [1] and sputtering [2], respectively, of metallic and organic components and inter alia allow the preparation of composites which contain alloy clusters of well defined composition. Emphasis will be placed on soft-magnetic high frequency materials with cut-off frequencies well above 1 GHz [3] and optical composites with tuned plasmon resonances suitable for ultra thin color filters, Bragg reflectors, and other devices [4-6]. In addition, antibacterial coatings [7] will be addressed. Moreover, a novel approach to produce magnetic nanorods for potential applications in high-density data storage and other fields will be presented [8].

[1] A. Biswas, Z. Marton, J. Kanzow, J. Kruse, V. Zaporojtchenko, F. Faupel, and T. Strunskus, Nano Letters, 3, 1, (2003).

[2] U. Schürmann, W.A. Hartung, H. Takele, V. Zaporojtchenko, and F. Faupel, Nanotechnology, 16, 1078, (2005).

[3] H. Greve, C. Pochstein, H. Takele, V. Zaporojtchenko, F. Faupel, A. Gerber, M. Frommberger, and E. Quandt, Appl. Phys. Lett. 89, 242501 (2006).

[4] A. Biswas, O. C. Aktas, U. Schürmann, U. Saeed, V. Zaporojtchenko, T. Strunskus and F. Faupel, Appl. Phys. Lett., 84, 2655, (2004).

[5] H. Takele, H. Greve, C. Pochstein, V. Zaporojtchenko and F. Faupel, Nanotechnology, 17, 3499, (2006).

[6] H. Takele, U. Schürmann, H. Greve, D. Paretkar, V. Zaporojtchenko, and F. Faupel, Eur. Phys. J. Appl. Phys. (EPJAP), 33, 83, (2006).

[7] V. Zaporojtchenko, R. Podschun, U. Schürmann, A. Kulkarni and F. Faupel, Nanotechnology, 17, 4904, (2006).

[8] Henry Greve, Abhijit Biswas, Ulrich Schürmann, Vladimir Zaporojtchenko, and Franz Faupel, Appl. Phys. Lett., 88, 123103 (2006).

IL-2

Metal Nanoclusters in Polymers of High Free Volume

Dr. Detlev Fritsch
Institut für Polymerforschung, GKSS-Forschungszentrum Geesthacht GmbH, Max-Planck-Straße 1, 21502 Geesthacht

By reason of limited possibility of close chain packing polymers exhibit a measurable part of volume unoccupied by the polymer chains, the so called Free Volume. For most common polymers the fraction of free volume varies only slightly. However, with special polymer design such as improving chain stiffness, decreasing chain interaction and incorporating bulky groups the free volume can be increased to a much higher level even close to the presence of end-to-end extension of same of the free volume. Up to today, only a few polymers with a level of free volume much above that of common polymers are known: i.e. polyacetylenes, Teflon® copolymers with cyclic perfluoroethers, PIM polymers (ladder polymers with a side of contortion and a silylated polynorbornene. We applied the method of co-solving a metal salt and a polymer followed by film formation and chemical reduction of the salt to metal nanoclusters with three high free volume polymers. The obstacles for generation of uniformly distributed Pt and Pd nanoclusters as well as the advantage of the nanoclusters incorporated into high free volume polymers will be presented and discussed.

IL-3

Introduction of Inorganic Components into Polymer Using Iodine

Yasuo Gotoh[1)], Akio Kawaguchi[2)], Yoshie Fujimori[1)], Yutaka Ohkoshi[1)], Masanobu Nagura[1)]
1) Faculty of Textile Science and Technology, Shinshu University, 3-15-1 Tokida, Ueda, Nagano 386-8567, JAPAN.
2) Research Reactor Institute, Kyoto University, Kumatori, Sennan-gun, Osaka 590-0494, JAPAN.
E-mail : ygotohy@shinshu-u.ac.jp

High-function and high-performance materials are demanded in various fields such as energy-saving, resource-saving, optics, and electrical and electronic engineering. Organic/inorganic hybrid or nanocomposite materials have been actively developed to obtain new properties that each component does not show independently. Representative of such materials is nanocomposite materials composed of inorganic nanoparticles introduced into an organic polymer matrix.

Numerous preparation procedures of nanocomposites have been developed by many researchers. We have utilized iodine as a precursor of inorganic component for preparing organic/inorganic composites [1,2]. Iodine can penetrate many kinds of polymer matrices, and form polyiodid-polymer complex. Iodine can form complex crystal with some polar polymers such as starch, polyvinyl alcohol, and nylon 6. Polyiodide ions (e.g. I_3^- and I_5^-) sorbed in a polymer matrix are reacted with metal ions such as gold, silver, and copper, consequently particles of semiconducting metal iodides of AuI, AgI and CuI are *in-situ* precipitated in the matrix. All procedures are wet processes; firstly polymer base materials are immersed in I_2-KI sokution, then polyiodide-polymer complexes are formed, and secondary, the complexes are reacted to metal ions in the corresponding metal ions aqueous solutions. After washing with distilled water and drying, the composites are obtained. The amount of the introduced metal iodides can be relatively easily controlled by the concentration of the immersion solutions, and immersion time and temperature. The iodides are introduced into the inner part of polymer matrix, and the dispersion state of the iodides is influenced by the orientations of matrix polymer and sorbed polyiodide ions. In the case of non-polar polymers, the iodine component can be introduced into the matrix by immersion in I_2-KI solution at high temperature higher than glass transition temperature of matrix polymer. Thus, the many polymers can be applied to metal iodide-polymer composites.

Some properties of nylon 6-AgI composite we prepared are interesting and different from that of the bulk AgI. For example, the conductivity of the composite having 15vol% β-AgI was approximately $10^{-5}\ \Omega^{-1}\mathrm{cm}^{-1}$, which is higher than that of neat AgI ($3\times10^{-7}\ \Omega^{-1}\ \mathrm{cm}^{-1}$). The crystal transition temperature of AgI was more than 20 °C lower than that of neat AgI, which is attributed to the excess of Ag^+ ions in the composite.

Some of the composites shows strong antibacterial properties against *Staphylococcus aureus*, *Klebsiella pneumoniae* and *Pseudomonad aeruginosa* as shown in Table 1. Metal iodides used in this study are very insoluble in water and are introduced into the inner part of fibers and plastics, thus the antibacterial property can be expected to be persistent for long time use.

Table 1 Antibacterial property of nylon 6 and nylon 6-AgI composite.

Kinds of bacteria	Colony forming unit (CFU / ml)			
	nylon 6 (control)		nylon 6-AgI	
	Initial	After 18 h	Initial	After 18 h
Staphylococcus aureus	8.85×10^3	2.44×10^6	8.85×10^3	10 >
Klebsiella pneumoniae	3.87×10^4	4.30×10^7	3.87×10^4	10 >
Pseudomonas aeruginosa	4.24×10^4	2.51×10^8	4.24×10^4	10 >

References

[1] Gotoh, Y.; Kanno, T.; Ohkoshi, Y.; Nagura, M.; Akamatsu, K.; Mizuhata, M.; Deki, S. Proceedings of International Synposium on Small Particles and Inorganic Cluster, 11, 11, B-XII-8, Strasbourg, 2002.

[2] Fujimori, Y.; Gotoh, Y.; Tamaki, N.; Ohkoshi, Y.; Nagura, M. J Mater Chem 2005, 15, 4816.

IL-4

Pt Modified with RuO_2 Nanosheets as Improved Fuel Cell Electrocatalysts

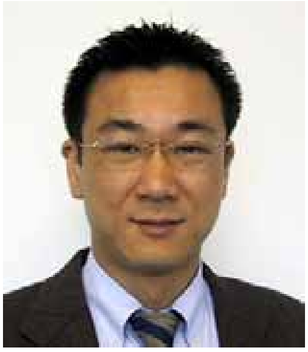

Wataru Sugimoto, Takahiro Saida, Yoshio Takasu
Department of Fine Materials Engineering, Faculty of Textile Science and Engineering, Shinshu University, 3-15-1 Tokida, Ueda, Nagano, 386-8567 JAPAN
E-mail : wsugi@shinshu-u.ac.jp

Fuel cells are considered to be one of the key technologies for the coming hydrogen economy. Carbon supported platinum alloys (PtM/C) are currently used as both anodes and cathodes in fuel cells operating at low temperatures such as direct methanol fuel cells and polymer electrolyte membrane fuel cells. PtRu/C is widely used as the anode catalyst, due to the promotional effect of Ru for the oxidation of adsorbed carbon monoxide (CO_{ad}) on Pt by supplying an oxygen source (Ru–OH_{ad}) and its ability to alter the electronic state of Pt. In the cathode catalyst layer, the poor kinetics of the oxygen reduction reaction and the lack of sufficient durability of the catalysts are two of the primary issues that need to be resolved for commercialization of fuel cells operating near room-temperature. Various binary alloys and Pt/oxides have been proposed as effective catalysts for for anode and cathode catalysts.

Despite the large amount of studies on Pt-based electrocatalysts, work is still needed to increase the specific activity, lower the catalyst loading and increase the durability. In particular, recent work has revealed that catalyst degradation is a major problem under fuel cell operating conditions. Thus, one must design electrocatalysts with high activity with sufficient durability.

Here we will report a possible approach to these problems; the modification of Pt/C with a polymeric inorganic macro anion, that is, hydrous ruthenic acid nanosheets (HROns).[1] The new electrocatalyst is based on Pt/C modified with RuO_2 nanosheets. The protonated RuO_2 nanosheets are derived by chemical exfoliation of a crystalline layered ruthenic acid ($H_{0.2}RuO_{2.1}\cdot nH_2O$), and is a nano-structured material with thickness of 0.4 nm and lateral size in the micrometer order. Originally developed for supercapacitor application, it possess excellent stability in a wide electrochemical window, high electroconductivity via the crystalline framework and proton conductivity via surface Ru-OH.[2]

The HROns colloid was prepared by intercalation-exfoliation reactions, and Pt/C was prepared by an impregnation method according to previous literature.[2,3] Pt/C powder was added to a

HROns colloid (Pt:Ru=1:0.5 molar ratio) and dried to a powder state. The prepared HROns-Pt/C catalyst was dropped onto a mirror-polished glassy carbon surface and a Nafion solution was used to stabilize the material. Electrochemical studies were conducted in a three-electrode cell with 0.5 M H_2SO_4 or O_2-saturated 0.5 M H_2SO_4 typically at 60°C. Durability tests were conducted by consecutive cycling.

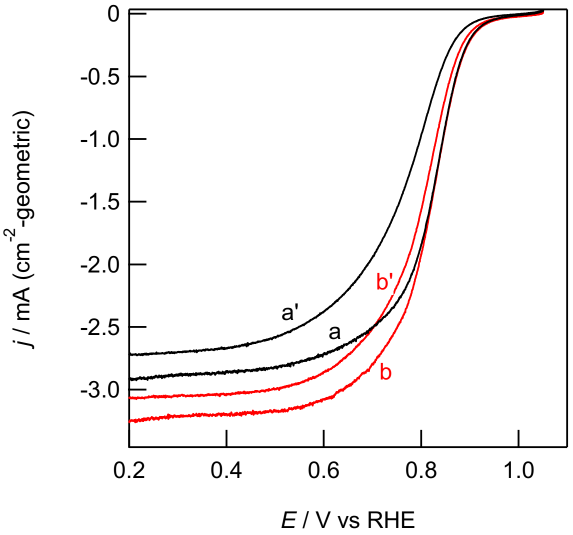

Figure 2. Hydrodynamic voltammogram in O_2-saturated 0.5 M H_2SO_4 (ω=2,000 rpm, v=5 mV s^{-1}). (a) Initial Pt/C, (a') Pt/C after durability test, (b) initial HROns-Pt/C, (b') HRO-ns-Pt/C after durability test. (a)(a'): 15.3 μg-Pt/cm^2, (b)(b') 13.9 μg-Pt/cm^2.

The modification of Pt/C with RuO_2 nanosheets resulted in an increase in both CO and CH_3OH electro-oxidation. Since neighboring OH species are need for the electroxidation of CO and CH_3OH, it is obvious that HROns acts as an efficient co-catalyst towards these reactions. Furthermore, consecutive cycling revealed a marked enhancement in durability by the modification with HROns (Fig. 1). After durability tests, the CH_3OH oxidation activity decreased to 18% of the initial activity. On the other hand, HROns-Pt/C maintained 55% of the initial activity. When used as a cathode catalyst, HROns-Pt/C exhibited slightly enhanced O_2 reduction activity. This is attributed to an increase in the electrochemically active Pt surface area by the modification and the possible participation of HROns to O_2 reduction. After durability tests in O_2-saturated electrolyte, the O_2 reduction activity decreased only to 74% of the initial activity for HROns-Pt/C, in comparison to 41% for Pt/C (Fig. 1).

These results clearly show that the modification of Pt/C with HROns not only increases the activity towards fuel cell related reactions, but the catalyst degradation is exceptionally retarded. Further enhancement in catalytic activity is anticipated by using HROns modified binary catalysts. Since ruthenium is present in a crystalline state in HROns-Pt/C, this composite material should show better stability compared to most metal alloy catalysts.

[1] W. Sugimoto, T. Saida, Y. Takasu, *Electrochem. Commun.*, **8**, 411 (2006).

[2] W. Sugimoto, H. Iwata, Y. Yasunaga, Y. Murakami, Y. Takasu, *Angew. Chem. Int. Ed.*, **42**, 4092 (2003).

[3] Y. Takasu, T. Fujiwara, Y. Murakami, K. Sasaki, M. Oguri, T. Asaki, W. Sugimoto, *J. Electrochem. Soc.*, **147**, 4421 (2000).

IL-5

Chemical Route to Synthesize Metal/Polymer Nanocomposites with Controlled Microstructures

Kensuke Akamatsu
Faculty of Science and Engineering, Konan University,
8-9-1 Okamoto, Higashinada, Kobe 658-8501, Japan,
and
PRESTO, Japan Science and Technology Agency (JST),
5 Sanbancho, Chiyoda-ku,Tokyo 102-0075, Japan

E-mail : akamatsu@center.konan-u.ac.jp

Nanocomposites consisting of polymer films containing metal nanoparticles have been expected to be useful for applications to novel electrical, magnetic, catalytic, and nonlinear optical materials and devices. In these applications, control of composite microstructures, which determines physical properties of the composites, is extremely important. Recently, in situ synthesis of metal nanoparticle/polymer composites by the process of dissolution and reduction of metal salts/or complexes within polymeric precursor films has been proposed. The advantage of this process is the uniform distribution of the metal source and the structural homogeneity of the precursors, which provides a resultant homogeneous dispersion of nanoparticles in polymer matrix. In this contribution, our latest findings on preparation of polymer nanocomposite containing metallic nanoparticles and control over their microstructures including nanoparticle size and volume fraction of metal phase will be presented. A major long-term goal of our research in this area is to develop ways of tailoring the design and formation of new nanocomposite materials with precisely controlled microstructures. Such the control over the parameters in the nanocomposites not only is an important for fabricating high performance nanocomposites of chosen functions but also should lead to fundamental understanding of the relationship of the physical properties to the composite microstructures.

OP-6

Photoinduced Hydrogen Production with Carotenoid-chlorophyll-platinum Nano-conjugated Micellar System

Yutaka Amao[1)], Yoshiko Fuchino[1)]

[1)] Department of Applied Chemistry, Oita University, Dannoharu 700, Oita, Japan

E-mail : amao@cc.oita-u.ac.jp

Light-harvesting site in photosynthesis protein consists of Mg chlorophyll-*a*, *b* (MgChl-*a*, *b*) and carotenoid dye such as β-carotene. MgChl-*a* and *b* plays an important role in photosynthesis such as light harvesting, the photoinducued electron transfer and so on. On the other hand, carotenoid dyes also have important functions such as the absorption of UV light, photo-protection of MgChl-*a* and *b*, photosynthesis protein and so on. In photosyhthesis protein, MgChl-*a*, *b* and carotenoid dyes are assembled via the hydrogen bond, hydrophobic interaction and coordination bond, not covalently. Thus, MgChl-*a*, *b* and carotenoid dyes can be assembled using hydrophobic interaction of surfactant micellar as photosynthesis protein mimetics.

In this work, artificial photosynthesis system, anionic water-soluble carotenoid dye crocetin (λ_{max} =536 nm) electrostatically immobilised onto the surface of cationic surfactant cetyltrimethylammonium bromide (CTAB) micellar including MgChl-*a* and *b* (Cro/MgChl), is prepared and its optical properties are investigated.

Cro/MgChl prepared as following method. At first, MgChl-*a* and *b* were solubilized in 20 mmol dm^{-3} cetyltrimethylammonium bromide (CTAB) micellar media containing potassium phosphate buffer (pH 7). Then, the crocetin solution containing potassium phosphate buffer (pH 7) was added to the MgChl-*a* and *b* solubilized CTAB micellar solution. The concentrations of crocetin, MgChl-*a* and *b* in Cro/MgChl are 0.43, 0.40 and 0.03 mmoldm^{-3}, respectively.

The fluorescence properties of Cro/MgChl ([Cro]=0.43 mmoldm^{-3}, [MgChl-*a*]=0.40 mmoldm^{-3}, [MgChl-*b*]=0.03 mmoldm^{-3}) were measured using a spectrofluorophotometer with a 150 W xenon lamp as a visible excitation light source (RF-5300PC Shimadzu). The excitation and emission bandpasses were 5.0 nm, respectively.

The photostability of MgChl-*a* and *b* in the Cro/MgChl was investigated. The sample solution containing Cro/MgChl ([Cro]=0.43 mmoldm^{-3}, [MgChl-*a*]=0.40 mmoldm^{-3}, [MgChl-*b*]=0.03 mmoldm^{-3}) : in 50 mmol dm^{-3} potassium phosphate buffer solution (pH 7.0) was deaerated by repeated freeze-pump-thaw cycles for 6 times. The reaction volume was 3.0 ml. A Philips KP-8 200W tungsten lamp at a distance of 3.0 cm (light intensity of 200 J $m^{-2}s^{-1}$) was used as steady state light source. The degradation of MgChl-*a* and *b* was estimated using the absorbance changes of Q bands of chlorophylls at 660 nm.

Figure 1 show the fluorescence emission spectrum of Cro/MgChl solution. Figure 1(a) show the fluorescence emission spectrum with excitation attributed to absorption band of crocetin (536 nm). The fluorescence at 680 nm due to MgChl-*a* and *b* is observed. However, the fluorescence at 572 nm due to crocetin is disappeared. In contrast, the fluorescence also is observed at 680 nm with excitation to absorption band of MgChl-*a* and *b* (660 nm) as shown in Figure 1(b). Moreover, the weak fluorescence at 680 nm is observed with 536 nm excitation in the CATB micellar including MgChl-*a* and *b* without crocetin (MgChl). These results indicate that the photoinduced energy transfer from the photoexcited state of crocetin to MgChl-*a* and *b* occurs.

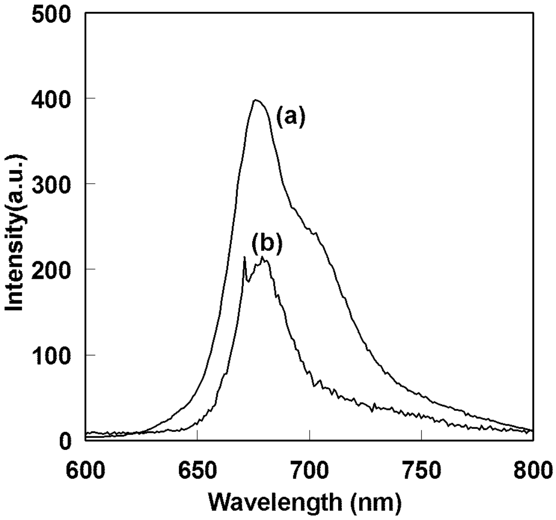

Fig. 1. Fluorescence emission spectrum of Cro/MgChl with excitation attributed to absorption band of crocetin (536 nm) (a) and to absorption band of MgChl-*a* and *b* (660 nm) (b).

Figure 2 shows the absorbance changes at 660 nm attributed to the absorption band of MgChl-*a* and *b* in Cro/MgChl with irradiation time. After 60 min irradiation, the absorbance decrease at 660 nm in Cro/MgChl and MgChl are 3.0 and 17 %, respectively. The absorbance decrease of MgChl-*a* and *b* in Cro/MgChl was slower than that of MgChl as shown in circle and square. These results indicate that the degradation rate of MgChl-*a* and *b* in Cro/MgChl against irradiation was suppressed by crocetin immobilization. As crocetin, which has a large absorption band less than 400 nm, absorbs the light of the wavelength less than 400 nm onto the surface of CTAB micelle including MgChl-*a* and *b*, the degradation of MgChl-*a* and *b* is suppressed.

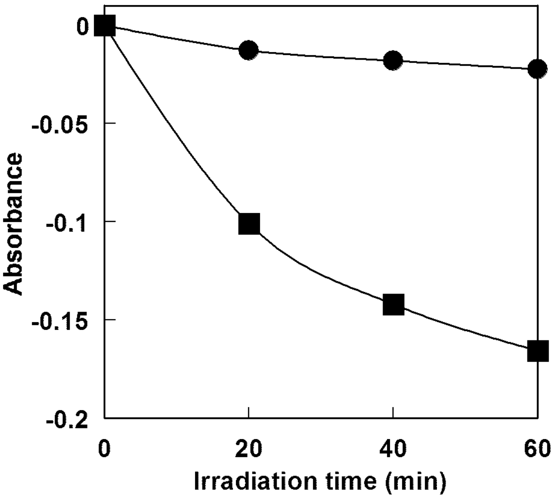

Fig. 2. Time dependence of absorbance changes at 660 nm attributed to MgChl-*a* and *b* in Cro/MgChl (circle) and MgChl (square) with irradiation.

OP-7

Title: Synthesis of palladium-LDPE nanocomposites by implantation of neutral clusters produced by a supersonic cluster source.

L. Ravagnan [1)], S. Rebasti [2)], G. Divitini [2)], V. Cassina [1)], P. Piseri [1)] and P. Milani [1)]

[1)] Dipartimento di Fisica and CIMAINA, Università di Milano,
Via Celoria 16, I-20133 Milano, Italy
[2)] Dipartimento di Fisica, Università di Milano,
Via Celoria 16, I-20133 Milano, Italy

E-mail : luca.ravagnan@mi.infn.it.

Supersonic cluster beam deposition is one of the techniques of choice for the synthesis of nanostructured films [1]. Its main advantages are high deposition rates and the possibility of exploiting aerodynamic focusing effects typical of supersonic expansions [2]. The usage of aerodynamic lenses in particular enables to decrease the cluster beam divergence up to less than 1° and then to be able to deposit patterns with high aspect ratio and controlled shapes by using micro-machined masks [3] (see Fig. 1).

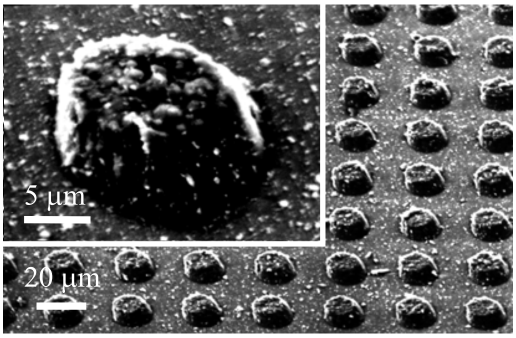

Fig. 1 SEM image of a pattern of pillars obtained with a round hole grid with 850 mesh and holes of 20 mm of diameter.

Recently we demonstrated how depositing a supersonic beam of palladium clusters produced by a Pulsed Microplasma Cluster Source (PMCS, [4]) on a low density polyethylene substrate at room temperature it is possible to implant the clusters (having kinetic energies to the order of 2 eV/atom) into the polymer matrix. This was detected by the characterization of the transport properties of the LDPE substrates during the clusters deposition. By studying the evolution of the film conductance as a function of the amount of deposited clusters we observed an insulator-conductor transition of the system that was well described by the classical percolation theory in a 3D system where metal particles are dispersed into an insulating medium. This result provides a first indication of palladium cluster implantation inside the polymer.

Above the percolation limit we furthermore observed an exponential growth of the film conductance with the amount of deposited cluster (Fig. 2a). We explained this unusual behavior (that could not be justified by tunneling between adjacent nanoparticles) by a statistical model describing the synthesis of the nanocomposite film, where the implantation of the nanoparticles is limited by their aggregation inside the polymer matrix with other nanoparticles already deposited. The results of this model (Fig. 2b) are in very good agreement with the experimental data, thus confirming the production of a nanocomposite.

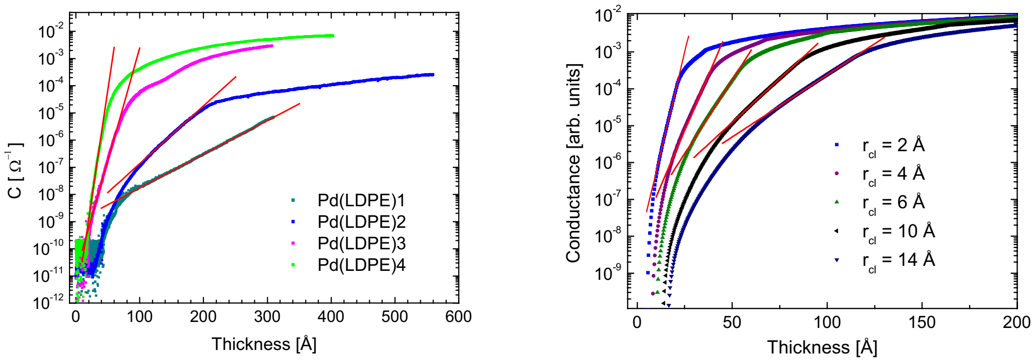

(a) (b)

Fig. 2 (a) Evolution of the conductance of the polyethylene-palladium nanocomposite during the cluster deposition as a function of the amount of deposited clusters. (b) Numerical simulation of the evolution of the conductance during the growth of the nanocomposite.

The possibility of synthesizing metal-polymer nanocomposites at room temperature by implantation of neutral clusters in a polymeric substrate opens new perspectives for the production of polymer based electronic devices, since supersonic cluster beam deposition enables to deposit micrometric patterns in batch and is a dry technique compatible with the high cleaning standards of the semiconductor industry.

References

[1] P. Milani and S. Iannotta. Cluster beam synthesis of nanostructured materials. Springer (Berlin), 1999.

[2] K. Wegner, P. Piseri, H. Vahedi Tafreshi, P. Milani. Cluster beam deposition: a tool for nanoscale science and technology. J. Phys. D: Appl. Phys. **39** , R439 (2006).

[3] E. Barborini, P. Piseri, A. Podestà, P. Milani. Cluster beam microfabrication of patterns of three-dimensional nanostructured objects. Appl. Phys. Lett. **77**, 1059 (2000)

[4] E. Barborini, P. Piseri, P. Milani. A pulsed microplasma source of high intensity supersonic carbon cluster beams. J. Phys. D: Appl. Phys. **32**, L105 (1999)

OP-8

Investigation of sol-gel templated polymer nanocomposite films for photovoltaic applications

J. Perlich[1)], M. Memesa[2)], Y.-J. Cheng[2)], J.S. Gutmann[2,3)], P. Müller-Buschbaum[1)]

[1)] TU München, Physik Department LS E13, James-Franck-Str.1, 85747 Garching (Germany)

[2)] Max-Planck Institute for Polymer Research, Ackermannweg 10, 55128 Mainz (Germany)

[3)] Institute of Physical Chemistry, University Mainz, 55099 Mainz (Germany)

E-mail : jan.perlich@ph.tum.de

The creation of nanostructured titania thin films has attracted considerable interest in the past years due to their physical properties associated with a variety of applications for example in coatings, photocatalysis, gas sensing and photovoltaics. In most of the applications the performance significantly depends on the morphology of the nanostructured titania, because the morphology determines the volume-to-surface ratio and hence the surface available for interfacial reactions. Moreover, in photovoltaics the morphology influences charge carrier transfer routes and thus electron-hole recombination probabilities. In order to accomplish the requirements arising from these versatile applications it is important to prepare the desired morphology with high reproducibility and homogeneously spread out over areas of cm^2.

For the preparation of the titania nanocomposite films we combine an amphilic diblock copolymer, which acts as the templating agent, with an inorganic sol-gel chemistry. Under these conditions a so-called good-poor-solvent pair induced phase separation leads to the formation of the nanostructures by film preparation via spin-coating on different substrates. Calcination at higher temperatures in air completes the preparation process comprising the rich capabilities of tailor-made morphologies [1].

The focus of this presentation will be on key parameters concerning the modification for an enhanced formation of nanostructures [2], the substrate properties such as the FTO-layer thickness (see figure 1) [3], and the thickness of the polymer nanocomposite films with respect to the desired morphology.

For the characterization of the nanostructured films in the different stages of preparation grazing incidence small angle x-ray scattering (GISAXS) is performed with synchrotron radiation (HASYLAB). GISAXS satisfies the requirement for a nondestructive method and enables to obtain morphological information of the thin film and its respective interfaces [4]. The structural characterization in real space is complemented by surface and thin film sensitive probes such as atomic force microscopy (AFM), x-ray reflectometry (XRR) and imaging ellipsometry.

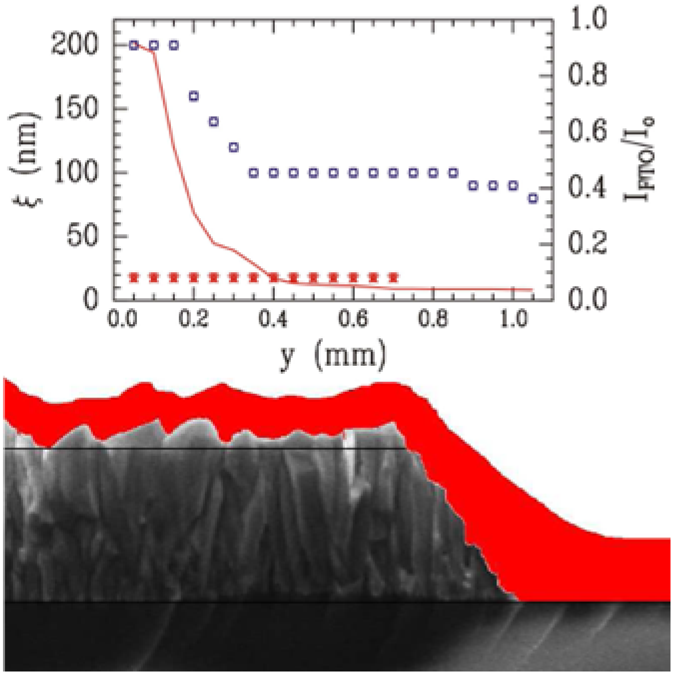

Fig.1: Detected characteristic lateral length of the FTO substrate layer (solid symbols) and of the nanocomposite film (open symbols) plotted as a function of the position in gradient direction y. For comparison the relative change in the FTO signal I_{FTO}/I_0 (solid line) is superimposed to show the gradient position. The subjacent sketch shows the gradient coated with the polymer nanocomposite layer.

This work was financially supported by DFG in the priority program SPP1181 (GU771/2 and MU1487/5).

References

[1] Y.-J. Cheng, J.S. Gutmann: *Morphology phase diagram of ultrathin anatase TiO_2 films templated by a single PS-b-PEO block copolymer*; J. Am. Chem. Soc. **128**, 4658 (2006)

[2] J. Perlich, L. Schulz, M.M. Abul Kashem, Y.-J. Cheng, M. Memesa, J.S. Gutmann, S.V. Roth, P. Müller-Buschbaum: *Modification of the morphology P(S-b-EO) templated thin TiO_2 films by swelling with PS homopolymer*; Langmuir, submitted

[3] P. Müller-Buschbaum, J. Perlich, M.M. Abul Kashem, L. Schulz, S.V. Roth, Y.-J. Cheng, J.S. Gutmann: *Combinatorial investigation of nanostructures formed in a titanium dioxide based nanocomposite film on top of fluor-doped tin oxide layers*; phys. stat. sol. (RRL) **1 (3)**, 119 (2007)

[4] P. Müller-Buschbaum: *Grazing incidence small-angle x-ray scattering – an advanced scattering technique for the investigation of nanostructured polymer films*; Anal.Bioanal.Chem. **376**, 3 (2003)

IL-9

Structure and morphology of nanostructured noble metal-polymer bilayers for optical applications

Stephan V. Roth[1)], Rainer Gehrke[1)], Georg Jakopic[2)], Ralf Röhlsberger[1)], Harald Walter[3)], Ralph Domnick[4)], Mottakin Abul-Kashem[5)], Peter Müller-Buschbaum[5)]

[1)] DESY, Notkestr. 85, D-22607 Hamburg, Germany
[2)] Joanneum Research, Franz-Pichler-Straße 30, A-8160 Weiz, Austria
[3)] CSEM SA, Badenerstrasse 569, CH-8048 Zürich, Switzerland
[4)] Ara-Coatings GmbH & Co. KG, Gundstr. 13, D-91056 Erlangen, Germany
[5)] TU München, Physik-Department LS E13, James-Franck-Str. 1, D-85748 Garching, Germany

E-mail : stephan.roth@desy.de

Noble metal-polymer nanocomposites are important materials in science and technology with a wide field application [1, 2]. This includes optical data storage, solar cells and anti-counterfeiting technology [1, 2, 3]. In all these applications the distinct optical properties of the noble metal nanoparticles in combination with the polymer (spacer) layer are exploited. These optical properties stem from the confinement of the free electron gas inside the nanometer-sized metal particles, leading to the so-called plasmon resonances and distinct absorption bands in the visible light.

For the investigations presented here, we advanced two-fold. Firstly, we explored a way to impose a superstructure on the noble metal nanoparticle layer by prestructuring the polymer substrate. We exploited here the wide variety of morphologies of the polymer layer using a blend of PS and PI. Two metals were applied, namely Au and Cu. In addition, we installed on each sample a one-dimensional gradient, a common technique for combinatorial studies, allowing for installing different morphologies on one single substrate [6, 7].

One method of choice for combinatorial studies is microbeam grazing incidence small-angle x-ray scattering (μGISAXS). We installed a microbeam at the HASYLAB beamline BW4 using compound refractive lenses in combination with a GISAXS setup to scan the gradient samples [8]. In order to analyze the data, we fitted and simulated two-dimensionally the data. Fig. 1 shows an example for the Au gradient. The agreement between data and simulation is excellent.. The simulations reveal, that the Au nanoparticle layer reproduces the polymer blend island structure, while for the Cu layer no roughness replication is found. Furthermore, we compare the results for the nanoparticle morphology with optical microellipsometry measurements and atomic force microscopy.

Secondly, we performed first in-situ sputtering studies using μGISAXS at BW4. Here, we investigated the vertical and lateral growth kinetics of Au-based nanocomposites. We present first results focussing on different stages of structure formation.

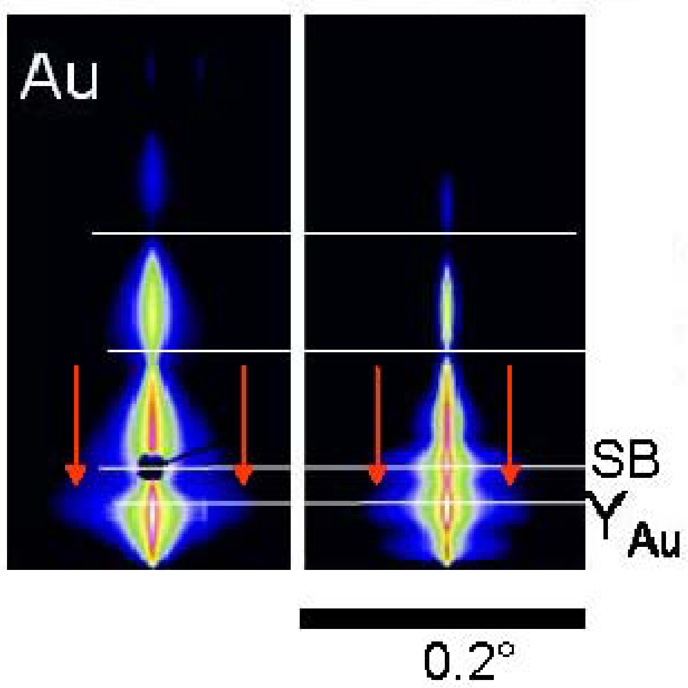

Fig.1: Left: μGISAXS data. Right: Fit using the IsGISAXS-Software [9]. SB denotes the point-like specular beam stop, Y_{Au} the Yoneda peak of Au. The vertical arrows indicate the in-plane structure and form factor of the Au nanoparticles, the horizontal lines the corresponding height form factor.

References

[1] A. Biswas, P.C. Karulkar, H. Eilers, M. Grant Norton, D. Skorski, C. Davitt, H. Greve, U. Schürmann, V. Zaporojtchenko, and F. Faupel, Vacuum Technology & Coating **7**, 54 (2006).

[2] U. Schürmann, H. Takele, V. Zaporojtchenko, and F. Faupel, Thin Solid Films **515**, 801 (2006).

[3] G. Bauer, J. Hassmann, H. Walter, J. Haglmüller, C. Mayer, and T. Schalkhammer, Nanotechnology **14**, 1289 (2003).

[6] S.V. Roth, H. Walter, M. Burghammer, C. Riekel, B. Lengeler, C. Schroer, M. Kuhlmann, T. Walther, A. Sehrbrock, R. Domnick, P. Müller-Buschbaum, Appl. Phys. Lett. **88**, 021910 (2006)

[7] S.V. Roth, M. Burghammer, C. Riekel, P. Müller-Buschbaum, A. Diethert, P. Panagiotou, Appl. Phys. Lett. **82**, 1935 (2003)

[8] S.V. Roth, R. Döhrmann, M. Dommach, M. Kuhlmann, I. Kröger, R. Gehrke, H. Walter, C. Schroer, B. Lengeler, P. Müller-Buschbaum, Rev. Sci. Instr. **77**, 085106 (2006)

[9] R. Lazzari, J. Appl. Cryst. **35**, 406 (2002)

IL-10

Physicochemical Properties and Applications of Polymer-Metal Nanocomposite Films near the Percolation Threshold

V. Zaporojtchenko, H. Takele, H. Greve, C. Hanisch, L. Li,
V.S.K. Chakravadhanula, A.Kulkarni, T. Strunskus and F. Faupel
Chair for Multicomponent Materials, Technical Faculty of the CAU Kiel, Kaiserstrasse 2, D-24143 Kiel, Germany

The present talk reviews properties of polymer-metal nanocomposite films (PMNF) with high volume fractions of metal nanoparticles close to the percolation threshold. In this regime, the d.c. electrical conductivity and the permittivity are extremely sensitive on the nanoparticle concentration and separation. The morphology of the nanocomposites (particle size and distribution) which were prepared by PVD methods, depend on the polymer and metal properties as well as on the preparation parameters like deposition rate and substrate temperature. As a consequence, a percolation threshold in the conductivity was observed at different critical concentrations of nanoparticles ranging from 15 to 40 vol. %. It is shown also that optical, magnetic and chemical properties may be varied strongly close to percolation. Thus the index of refraction can be tuned over a wide range, and surface plasmons, occurring for noble metals in the visible range, can be shifted to the infrared regions. Concerning the potential application of the PMNF near the percolation threshold, in this talk, emphasis is put on electromagnetic, optical, chemical, and biosensors. PMNF as chemical sensors operate on the principle of swelling of the polymers in the presence of organic vapors and take advantages of the strong dependence of physical properties near the percolation threshold on in cluster separation which changes due swelling. Moreover, a novel approach, based on photochromic polymer–metal composites is discussed.

IL-11

Magnetic and structural properties of thin polymer films with embedded super-paramagnetic γ-Fe2O3 nano-particles

M.M. Abul Kashem, J. Perlich, L. Schulz, P. Müller-Buschbaum

TU München, Physik Department LS E13, James-Franck-Str.1, 85747 Garching (Germany)

Polymer nano-structures with incorporated magnetic nano-particles mark a new class of composite materials. Composite structures are formed from a matrix (polymer) and magnetic filler (e.g. metal or metal oxide or alloy). The polymer nano-structures, acting as a template, enable a completely new arrangement of the particles which is inaccessible with common magnetic materials. The controlled incorporation of the particles results from the presence of a hairy polymer layer covering the magnetic particles [1]. The chemical design of this coating is a key feature in the creation of the organic-inorganic composites.

On top of solid supports the polymer layers including particles are prepared by spin-coating. The nano-structures are created by the interplay of dewetting, macro- and micro-phase separation [2]. Within this self-assembly process the polymer matrix and the magnetic particles are ordered. The resulting structures and the magnetic properties are investigated.
The structural characterisation is based on real space techniques such as atomic force microscopy (AFM) or transmission electron microscopy (TEM) as well as on scattering techniques using neutrons (FRM-II, ILL) and synchrotron radiation (ESRF, HASYLAB). With grazing incidence small angle scattering (GISAS) the lateral arrangement of the polymer matrix and of the incorporated particles is determined.

Magnetization measurements at 2 K and 300 K show that the saturation magnetization is linear dependent on the nano-particle concentration. A constant coercitive field and increasing fields of remanence for different nano-particle concentrations are verified. AC-susceptibility measurements exhibit non-interacting super-paramagnetic behavior of the nano-particle ensemble [3].

[1] V.Lauter-Pasyuk, H.J.Lauter, G.P.Gordeev, P.Müller-Buschbaum, B.P.Toperverg, M.Jernenkov, W.Petry: *Nanoparticles in diblock copolymer films investigated by off-specular neutron scattering*; Langmuir **19**, 7783 (2003)
[2] M.M.Abul Kashem, J.Perlich, L.Schulz, S.V.Roth, W.Petry, P.Müller-Buschbaum: *Maghemite nanoparticles on supported diblock copolymer nanostructures*; Macromolecules, at press
[3] L.Schulz, S.Vallopilly, W.Schirmacher, P.Böni, W.Petry, P.Müller-Buschbaum: *Magnetic properties of thin diblock copolymer films with embedded γ-Fe2O3 nanoparticles*; Phys. Rev. Lett. submitted

IL-12

Characteristics of Scattering Photons from a Small Number of Molecules at Metal Nanogap

Kei Murakoshi, Yoshitaka Sawai, Mai Takase, Hideki Nabika
Division of Chemistry, Graduate School of Science,
Hokkaido University, Sapporo 060-0810, Japan
E-mail: kei@sci.hokudai.ac.jp

Nano-sized plasmon active metal dimer becomes to show intense surface-enhanced Raman scattering (SERS) when its distance is well-controlled. Recently, we have succeeded in optimizing the structure of Ag dimer arrays for the observation of intense SERS from a small number of isolated molecules at the SERS active sites (Figure 1). This highly SERS active site at metal nano-gap is expected to provide a chance to observe and/or clarify novel characteristics of SERS spectrum. As very unique characteristics of SERS, relatively strong anti-Stokes (aS) scattering intensity have been collected much attention, because of the expectation for observation and control of the vibrational population of molecules. In the present study, the Ag dimer array showing intense SERS was prepared to obtain characteristics of aS/S ratio of SERS photons. Well-reproducible spectrum in single-molecule level from the single SERS active site can offer the chance for detailed analysis of the aS/S ratio to clarify the origin. The aS/S ratio of the SERS spectrum was determined via continuous measurement of certain SERS active site. Typical features of SERS and normal (un-enhanced) Raman scattering spectra both in aS and S regions were shown in Figure. Normal (un-enhanced) Raman scattering spectrum was obtained using solid 4, 4'-bipyridine sample. As the wavenumber of the band becomes higher, it was fond that relative intensity of the aS band of the normal Raman decreases. This normal wavenumber dependence was changed at the SERS spectra (Figure 2 (b)-(c)). Relative intensities of the bands were significantly dependent

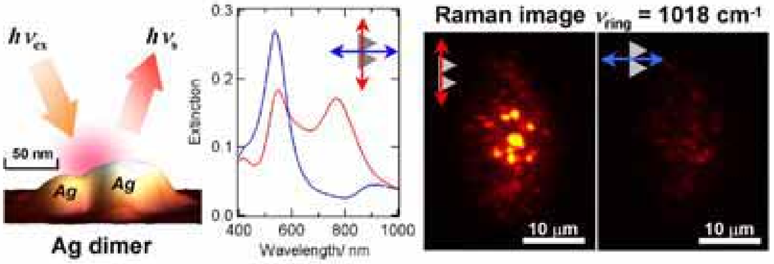

Figure 1. AFM image of Ag dimer; polarized extinction spectra and Raman images of the Ag dimer array.

upon observed area. At the SERS spectrum shown in Figure 2 (c), the aS bands around 1600 cm^{-1} are not clear, compared with the band at 1018 cm^{-1}. However, the intensities of the aS bands around 1600 cm^{-1} in Figure 2 (b) and (d) are comparable to those between 1200 cm^{-1} and 1400 cm^{-1}. The contribution of collective plasmon resonance of metal structure and coupled plasmon-resonance of molecules cannot explain the difference of the aS and S spectral features, because of the fact that the energy difference between the bands is relatively small compared with intrinsic energy width of the optical resonance. Both of the plasmon and the molecular states resonance have a few hundred meV band width at room temperature. Observed "selective" enhancement of specific aS band, whose energy difference with un-enhanced aS band is less than a few tens meV, cannot be explained by only optical resonance contribution. At the present stage, we do not have any definitive interpretation on the "selective" enhancement of specific aS band. There should be very specific vibrational band excitation available on the adsorbed molecules at highly localized electromagnetic filed. Information of the vibrational characteristics can be applied for ultra-sensitive analytical system as well as development of novel research for energy conversion technique controlling temperature of a single molecule. Further detailed spectral analysis of aS and S SERS photons from controlled adsorption molecules can provide information on the origin of the anomalous feature of the aS/S spectra

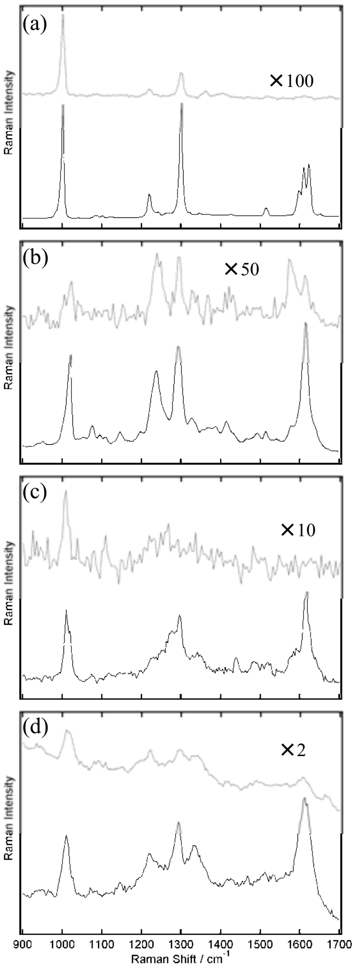

Figure. Stokes and anti-Stokes Raman spectra of solid 4,4'-bipyridine (a) and those observed at the periodic Ag dimer array in the 1 mM aqueous solution of 4,4'-bipyridine (b, c, d); I_{ex} = 200 mW , exposure time = (b, c) 2 s, (d) 100 s

References

1) Y. Sawai, B. Takimoto, H. Nabika, K. Murakoshi, *Can. J. Anal. Sci. Spec.*, **52**, 121 (2007).
2) Y. Sawai, B. Takimoto, H. Nabika, K. Ajito, K. Murakoshi, *J. Am. Chem. Soc.*, **129** 1658 (2007).
3) Y. Sawai, B. Takimoto, H. Nabika, K. Ajito, K. Murakoshi, *Faraday Discussions* **132**, 179-190 (2006).
4) N. Takeda and K. Murakoshi, *Anal. Bioanal. Chem.*, **388**, 103 (2007).

IL-13

Clean Synthesis of Highly Dispersed Metal Nanoparticles in Ionic Liquids Using a Sputter Deposition Technique

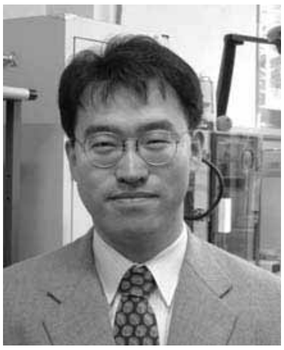

Tsukasa Torimoto,(1) Ken-ichi Okazaki,(1) Tomonori Kiyama,(1) Kaori Hirahara,(2) Nobuo Tanaka,(2) and Susumu Kuwabata(3)

(1) Graduate School of Engineering, Nagoya University, Chikusa-ku, Nagoya 464-8603, Japan

(2) EcoTopia Science Institute, Nagoya University, Chikusa-ku, Nagoya 464-8603, Japan

(3) Graduate School of Engineering, Osaka University, Suita, Osaka 565-0871, Japan

E-mail: torimoto@apchem.nagoya-u.ac.jp.

Synthesis of metal nanoparticles with a diameter of a few nanometers has attracted much attention, because the physicochemical properties of such particles were remarkably dependent on their size. In general these nanoparticles can be prepared in a solution by the reduction of the corresponding metal ions or metal complexes in the presence of additional stabilizing agents (e.g., thiol compounds and polymers). As a result, the prepared suspension contains byproducts, remaining substrates, and stabilizing agents. Since species other than metal nanoparticles are sometimes obstructive for utilization of the prepared nanoparticles, their removal is needed. Here we report an extremely clean method to synthesize gold (Au) nanoparticles in ionic liquids (ILs) using a sputter deposition technique without any additional stabilizing agents. The extremely low vapor pressure of ILs enables vacuum deposition of solid materials onto ILs. The simple sputter deposition of gold onto ILs resulted in the formation of a solution containing highly dispersed Au nanoparticles.[1]

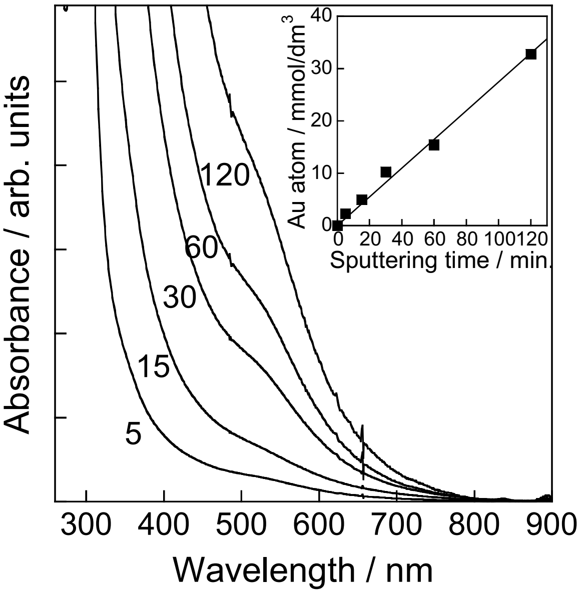

Fig. 1 Changes in the absorption spectra of EMI-BF4 with sputter deposition of Au. Sputtering time is shown in the unit of minutes in the figures. (inset) Concentration of Au in EMI-BF4 as a function of sputtering time.

A 0.60 cm^3 portion of 1-ethyl-3-methylimidazolium tetrafluoroborate (EMI-BF4) was spread on a glass plate (20 cm^2)

that was horizontally set in a sputter coater equipped with gold (99.99% in purity) foil target. Sputter deposition onto ILs was carried out with a current of ca. 4.0 mA under an air pressure of ca. 20 Pa at room temperature.

Figure 1 shows changes in the absorption spectra of EMI-BF4 with the sputter deposition of Au. Spectra showing onset around 800 nm and a shoulder around 520 nm assigned to the surface plasmon resonance (SPR) peak of Au nanoparticles developed with elapse of sputtering time. The concentration of Au in the IL was proportional to the sputtering time as shown in the inset of Fig. 1. It is well known that the SPR peak becomes remarkably sharp with an increase in the size of spherical Au nanoparticles from 2 to 9 nm. However, the peak shape of the spectra shown in Fig. 1 seemed to be invariable even when the Au concentration reached as high as 33 mmol dm^{-3} after 120 min of sputtering. This indicates that the successive sputtering did not cause any significant change in the size as well as size distribution of Au nanoparticles. Hence, a desired concentration of Au nanoparticles was simply obtained by adjusting the sputtering time.

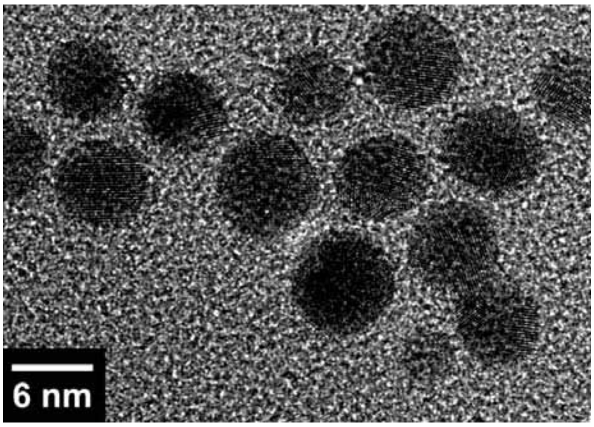

Fig. 2 TEM images of Au nanoparticles prepared by sputter deposition onto EMI-BF4

Figure 2 shows TEM images of Au-deposited EMI-BF4. Sputter deposition onto EMI-BF4 resulted in the formation of spherical nanoparticles that had clear lattice fringes with interplanar spacing of 0.24 nm assigned to the (111) plane of the face-centered cubic (fcc) crystal structure of gold. The average diameter of Au nanoparticles was determined to 5.5 nm with a standard deviation of 0.86 nm.

In conclusion, an extremely clean way to synthesize Au nanoparticles in IL was demonstrated using the sputter deposition technique. The deposited nanoparticles were very stable in the absence of any additional stabilizing agents. This could not be achieved by the vacuum deposition onto conventional organic liquids, in which the surface of metal particles must be modified with stabilizing agents to prevent the aggregation. This technique will also enable the preparation of alloy nanoparticles with simultaneous evaporation of different kinds of pure materials.

References

[1] T. Torimoto, K.-i. Okazaki, T. Kiyama, K. Hirahara, N. Tanaka, and S. Kuwabata, *App. Phys. Lett.*, **89**, 243117 (2006).

Chair Lecture -14

Novel Fabrication Process of Conductive Material / Metal Nanoparticle Composite for Electrode

Shigehito DEKI and Minoru MIZUHATA
Department of Chemical Science and Engineering,
Graduate School of Engineering,
Kobe University, 1-1 Rokkodai-cho, Nada, Kobe, 657-8501 Japan
E-mail : deki@kobe-u.ac.jp

Various kinds of new functional materials utilized for the electrochemical devices such as batteries, fuel cells and capacitors have been studied recently. Especially, since the electrode materials for polymer electrolyte fuel cells (PEFCs) require the highly electron conduction and transport of ionic species and supplied gases, the high performance of electrochemically high activity and durability for gas diffusion electrode. We have tried to improve the performance of the electrode with high dimensional reactive region using several kinds of techniques. In this paper, the novel fabrication processes are presented after previous studies[1)].

1. Carbon/highly dispersed Pt nanoparticles composite using heat-treatment of PAN matrix

For the improvement of the conductivity and electrode activity of carbon electrode for fuel cells, it is important to the control of the ratio of the carbon structure. The composite containing carbon graphite / Pt nanoparticles was fabricated by the heat-treatment of polyacrylonitrile (PAN). At first, PAN film was formed by vapor deposition method with the thickness of 100 nm. Deposited film was heat-treated a 230 ^{o}C for 3 hours in air flow for drying and eliminating the sample having lower molecular weight. The dried film was immersed into 5 mmol $Pt(NH_3)_6Cl_4$ aqueous solution for 10 hours at 40 ^{o}C. After platinum complex penetrated, the sample was heat-treated at 400, 600, and 800^{o}C for 10 minutes, respectively. Obtained sample was evaluated by TEM, XPS, FI-IR, and Raman spectroscopy. TEM image of obtained Pt/Carbon composite is shown in Fig.1. Each Pt particles are isolated and the average diameter is ca 2.5 nm with 0.4 nm of S.D. In the carbon matrix, the graphite region increased with the carbonized temperature. The polymer matrix of PAN influenced to the interaction between platinum nanoparticles during reducing reaction, and the graphite structure was formed by the catalytic effect of reduced platinum particles in the high temperature range. FT-IR spectra of heat-treated samples indicated that the absorption bands of $-(C{=}C)_x$- stretcheing band increased with the temperature as shown in Fig.2. It is suggested that the decomposition of PAN began at above 230^{o}C to ca 600^{o}C. According to Raman spectra, the intensity ratio of I_G/ I_D increased with the heating temperature as shown in Fig.3. It is suggested that the sp^2 bonding structure of carbon formed with the heating process in the reduced carbon from PAN films with the dispersed platinum.

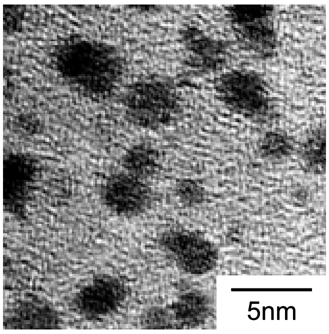

Fig. 1 TEM image of composite films after heat treatment at 600 ºC.

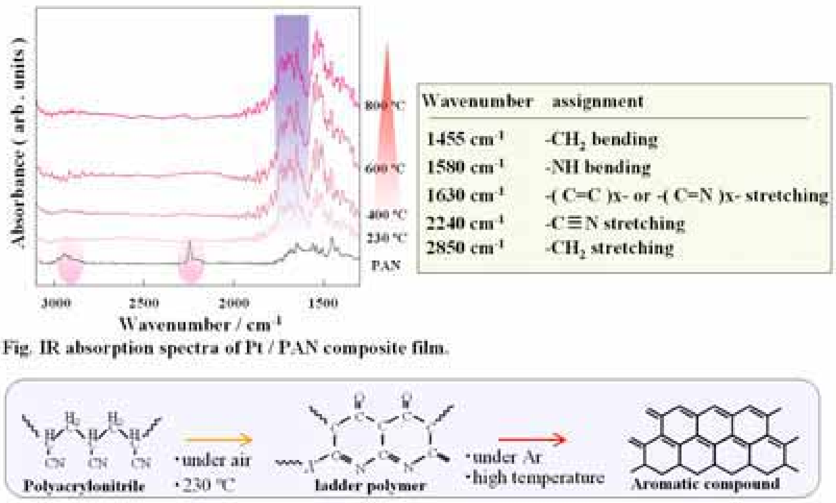

Wavenumber	assignment
1455 cm^{-1}	-CH_2 bending
1580 cm^{-1}	-NH bending
1630 cm^{-1}	-(C=C)x- or -(C=N)x- stretching
2240 cm^{-1}	-C≡N stretching
2850 cm^{-1}	-CH_2 stretching

Fig. IR absorption spectra of Pt / PAN composite film.

Fig.2. Carbonized process and corresponding FT-IR spectra during the heat-treatment of Pt/PAN composite.

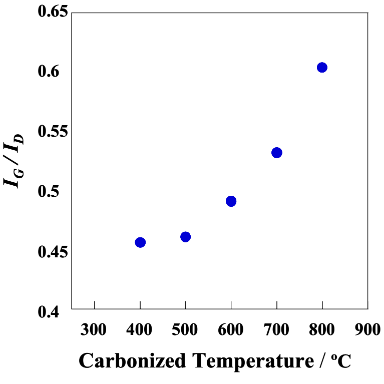

Fig. 3 Integrated intensity ratio of G band to D band as a function of carbonized temperature.

2. Preparation of Pt/Electro- conductive polymer loaded carbon composite[2)]

In the viewpoint of the electrode durability of polymer fuel cells, some studies intended that the platinum catalyst diffuse into the ion-exchange membrane by oxidation during the oxygen reduction at the open circuit voltage[3)]. It is necessary to prevent the coagulation and diffusion of the platinum catalyst and its shortage of the durability. We have attempted optimization of the reaction condition of Pt/PPy composite and measured the catalytic activity for oxygen reduction in order to make a high dimensional structure of the gas diffusion electrode[4)]. The oxidation of pyrrole (Py) into polypyrrole and the reduction of Pt(IV) to Pt(0) is proceeded using H_2PtCl_4 by the following reaction at room temperature. In previous study, we have presented the preparation method of Pt/polypyrrole composite loaded on surface oxidized carbon[3)]. In this study, the Pt/polypyrrole and Pt/polyaniline composites were loaded on the surface-oxidized carbon support using the similar reaction of the onestep synthesis of Pt/PPy and Pt/PANi composites. The durability and diffusion of Pt catalyst are discussed.

The preparation procedure is shown in Scheme 1. Vulcan XC-72R carbon powder was oxidized by High concentrated $KMnO_4$ and HNO_3 aqueous solution for 4 hours. Surface oxidized active group on carbon was ion-exchanged by the aqueous HCl solution for 20hrs. Resulting material has a ca 0.8 meq/g-carbon of the ion-exchange capacity. The surface acidic group was ion-exchanged by $[Pt(NH_3)_4]OH_2$ aqueous solution during neutralization. After drying, the Pt ionized carbon was put into the pyrrole aqueous solution. Immediately, the oxidation of platinum and polymerization of pyrrole or acidic aniline proceeded simultaneously.

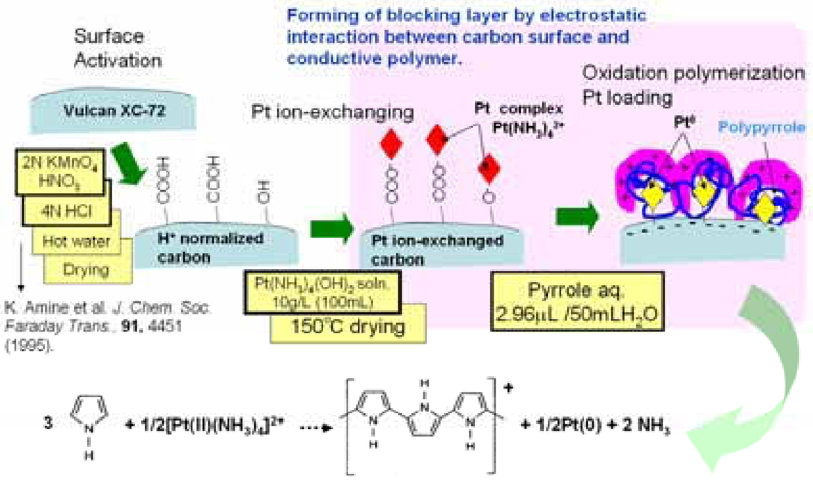

Scheme 1. Preparation procedure of Pt/PPy composite on oxidezed carbon.

The distribution of the platinum particles was measured by EDX equipped scanning microscope. In order to evaluate of catalytic activity of the composite, a cyclic voltammogram was measured for the Pt/polymer composite samples. Nafion® solution (5 wt%, Aldrich) was added to Pt/polymer-carbon composite as a binder. The composite was supported by the glassy carbon electrode. The electrode is set into 1mol/l H_2SO_4 aqueous solution with N_2 or O_2 bubbling.

Size distribution of loaded platinum particle ranged at 3-8 nm by TEM image observation. As a result of the reaction, Pt was loaded on carbon surface combined by the Polypyrrole uniformly as shown in Fig.4a. Polypyrrole laver covered carbon surface with platinum particles. It is suggested that the platinum particle was dispersed on the carbon paticles with polypyrrole polymer as shown in Fig.4b. Detail electrochemical properties will be discussed the other presentation[5)].

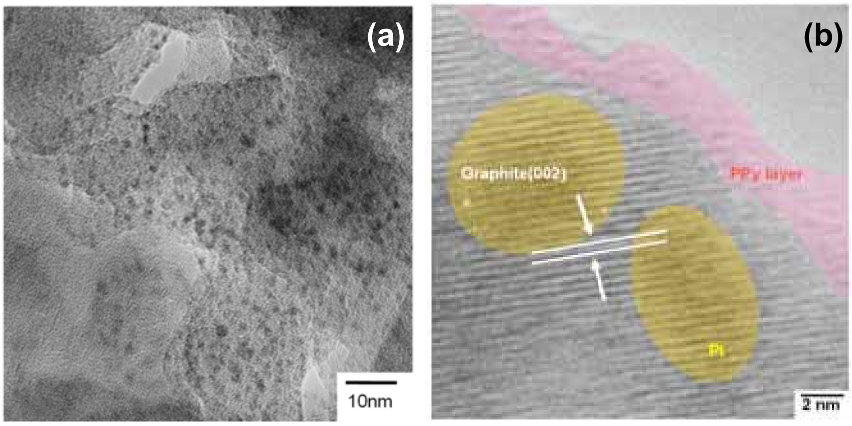

Fig. 4. (a) Well-dispersed Pt particles on oxidezed carbon with polymerized polypyrrole and (b) high-resolution image of the carbon surface with PPy.

References

1. H. Nabika, M. Mizuhata, A. Kajinami, S. Deki, K. Akamatsu, *J. Electroanal. Chem.*, **559(15)**, 99-102 (2003), which is presented at Nanoworkshop 2003 in Kiel.
2. M. Mizuhata, M. Oga, and S. Deki, *ECS Transaction*, **2(8)**, 63 (2007).
3. A. Taniguchi, T. Akita, K. Yasuda, and Y. Miyazaki, *J. Power Sources*, **130**, 42 (2004).
4. S. Deki, H. Nishikawa, and M. Mizuhata, *Electrochemistry*, **72(6)**, 415 (2004).
5. M. Oga, M. Mizuhata, S. Deki, Abstract of Nanoworkshop 2007 in Kobe, PS-10 (2007).

OP-15

In-situ observation of metal nanoparticle ordering at the air-water-substrate boundary in colloidal solutions

Stephan V. Roth$^{1)}$, Tina Autenrieth$^{1)}$, Gerhard Grübel$^{1)}$, Manfred Burghammer$^{2)}$, Christian Riekel$^{2)}$

$^{1)}$ DESY, Notkestr. 85, D-22607 Hamburg, Germany
$^{2)}$ ESRF, 6rue Jules Horowitz, F-38043 Grenoble Cedex 9, France

E-mail : stephan.roth@desy.de

Large-scale arrays of ordered nanoparticles are fascinating materials for science and technology, e.g. data storage [1] or DNA sensoring [2], due to their distinct optical properties [2-4]. To deposit the nanoparticle layer on top of the substrate, several methods are available, e.g. vacuum deposition [1,5] and solution casting. Nanostructuring using solution casting is one method of choice to install large-area two-dimensional (2D) thin films with specific morphology, offering the possibility to design 2D or three-dimensional (3D) photonic crystals. This method is especially important and applicable in the field of colloidal particles, as colloidal particles are often suspended in aqueous solutions.

The nanostructuring, however, is a very complex process involving several mechanisms [6]. Using a colloidal aqueous solution of two nanometer gold nanoparticles in water, the nanoscale structuring is followed during evaporation of a droplet on a silicon substrate including the structure formation at the three-phase contact line air-solution-substrate. We investigated the transfer of lateral order and vertical layering as a function of time at this three-phase contact line combining a nanometer-sized x-ray beam with a grazing incidence geometry. A pronounced retardation of vertical ordering is observed with respect to lateral ordering. Furthermore, individual layers are deposited during evaporation of the solvent, while the growth parallel to the substrate shows a strongly non-diffusive behavior. Fig. 1 shows shows the time-evolution of the nanostructure formation of the gold colloids during evaporation of the water. Clearly, a distinct retardation of the vertical ordering and growth with respect to lateral structuring is observed. This behaviour can be interpreted as clustering of nanoparticles and domain formation during evaporation of the solvent. The non-diffusive character of lateral clustering is emphasized by the power-law behavior and can be caused by convective flows, reducing the exponent. Furthermore, we will investigate the influence of the variation of the substrate, e.g. by using nanostructured polymer layers.

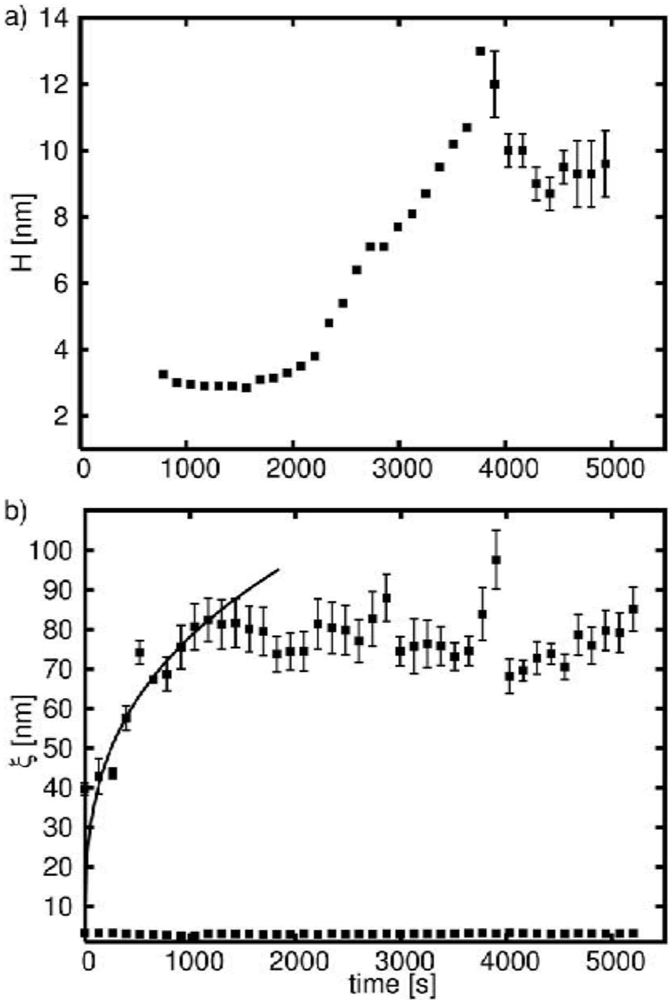

Fig.1: a) Quantitative analysis of the vertical layering of the gold colloids during water solvent evaporation. t=0s corresponds to the time, when the three-phase contact line (colloidal solution - air -substrate) arrives at the nanobeam position. For 780s $<t<$ 2000s, the layer thickness remains nearly constant. The subsequent increase stems from layer-by-layer deposition (one layer each 340 s). After the peak, compaction of the colloidal layer occurs, and the height stays constant.

b) Most-prominent in plane length scale ξ. $\xi(t)$ follows a $t^{0.32\pm0.06}$ power-law (solid line). The lower symbols indicate the radius of the spherical gold nanoparticles for comparison. Clearly, the layer-by-layer deposition is retarded with respect to the lateral nanostructuring.

References

[1] A. Biswas, P. Karulkar, H. Eilers, M. G. Norton, D. Skorski, C. Davitt, H. Greve, U. Schürmann, V. Zaporojtchenko, and F. Faupel, Vacuum Technology & Coating **7**, 54 (2006).

[2] G. Bauer, J. Hassmann, H. Walter, J.Haglmüller, C. Mayer, and T. Schalkhammer, Nanotechnology **14**, 1289 (2003).

[3] H. Ditlbacher, J. Krenn, B. Lamprecht, A. Leitner, and F. Aussenegg, Optics Lett. **25**, 563 (2000).

[4] A.-P. Hynninen, J. H. J. Thijssen, E. C. M. Vermolen, M. Dijkstra, and A. V. Blaaderen, Nature Mat. **6**, 202 (2007).

[5] S. V. Roth, H. Walter, M. Burghammer, C. Riekel, B. Lengeler, C. Schroer, M. Kuhlmann, T. Walther, A. Sehrbrock, R. Domnick, and P. Müller-Buschbaum, Appl. Phys. Lett. **88**, 021910 (2006).

[6] P. Müller-Buschbaum, E. Bauer, S. Pdister, S. V. Roth, M. Burghammer, C. Riekel, C. David, and U. Thiele, Europhysics Lett. **73**, 35 (2006).

IL-16

Properties of metal nanowires on polymers

Prof. Dr. Rainer Adelung

Lehrstuhl für Materialverbunde, Institut für Materialwissenschaft, Christian-Albrechts-Universität zu Kiel,
Kaiserstr. 2, D-24143 Kiel, Germany

Properties of metals change at the nanoscale. Gold and nickel nanowires on polymers show a very different conductivity behavior, response to magnetic fields or oxidation behavior than their macroscopic counterparts. For example, for small nanowire cross sections, a hopping dominated transport can be observed, leading to a conductivity increase at higher temperatures in contrast to bulk metallic behavior. By choosing a mesoscale wire thickness, a temperature independent conductivity can be found. Beside the presentation of these properties, different, simple methods will be presented that allow a large scale fabrication of metal or polymer nanowires on different substrates. Furthermore, effective strategies for the contact formation will be presented.

IL-17

Eco- & Nano-Polymer Composites

Takashi Nishino[1)], Masaru Kotera[1)],Yukari Sakagami[1)], Aya Nakai[1)]
Yoshimasa Urushihara[2)]
1) Department of Chemical Science and Engineering,
Graduate School of Engineering, Kobe University,
Rokko, Nada, Kobe 657-8501, Japan
2) Hyogo Science and Technology, Kouto, Kamigoori, Acho, Hyogo 678-1205, Japan
E-mail : tnishino@kobe-u.ac.jp

Polymer/clay nanocomposite, in which small amount of exfoliated silicate was highly dispersed in polymer matrix, shows remarkable improvements in mechanical and thermal properties, gas barrier properties and flame retardation [1,2]. For polymer/clay nanocomposites, Nylon system was first invented by Toyota Central R&D [3], and Unitika Ltd [4]. After being stimulated by these works, it has extended to polypropylene, polystyrene, polylactic acid, polyimide and thermosetting resin systems. Generally, preparation of polymer/clay nanocomposite is made use of organically modified clay, by which layered silicate is exfoliated through *in-situ* polymerization or intercalation of polymer. However, organic modifier causes some problems such as thermal coloring of nanocomposite, increments of process steps and cost. In addition, it is intrinsically environment-unfriendly even through the matrix resin is environmentally friendly.

Clays such as montmorillonite (MMT) are well known to swell in water and form stable aqueous suspension. So, by combination with water-soluble polymer, nanocomposite will be expected to be formed with unmodified clay. In this study, poly(vinyl alcohol) (PVA), the most popular water-soluble polymer, is selected as the matrix resin. PVA/MMT nanocomposite was prepared by simply casting PVA/MMT aqueous suspension. Theni structure, properties and orientation behavior of the nanocomposite were investigated. Especially, the effect of drawing on the structure and the elongation at break was focused.

Table 1 summarizes the advantages of introducing exfoliated MMT (5 wt%) for PVA system. As can be expected for the barrier effect of the MMT layers, thermal decomposition temperature increased, and water swelling ratio decreased. In addition, mechanical properties increased without losing optical transparency of PVA film. On the contrary, the elongation at break decreased from >100 % to <5 %, which results in the decrease of toughness of the composite. The decrease of the elongation at break is commonly observed, and it has been main issue for clay based nanocomposites.

Table 1 Advantages of PVA Nano & Eco Composite

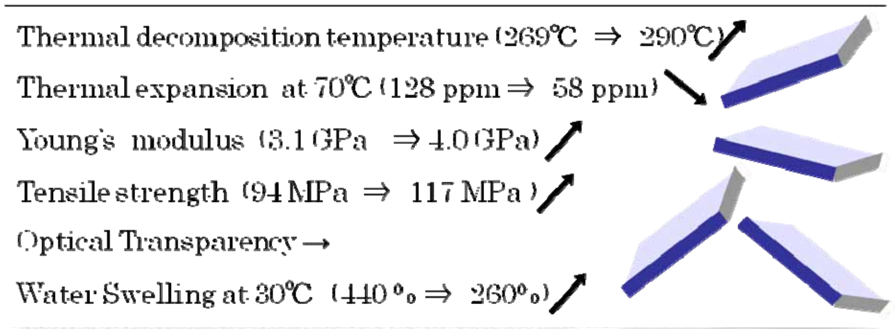

Thermal decomposition temperature (269℃ ⇒ 290℃) ↗
Thermal expansion at 70℃ (128 ppm ⇒ 58 ppm) ↘
Young's modulus (3.1 GPa ⇒ 4.0 GPa) ↗
Tensile strength (94 MPa ⇒ 117 MPa) ↗
Optical Transparency →
Water Swelling at 30℃ (440 % ⇒ 260 %) ↗

Fig.1 shows the stress-strain curve of PVA/MMT nanocomposite uniaxially drawn at 120℃. By drawing, in general, the tensile strength and modulus increase and the elongation at break decreases. However, the elongation at break increased for the nanocomposite, which corresponds to the increase of toughness of over 12 times. In order to investigate this phenomenon, we investigated MMT and PVA orientation using synchrotron X-ray diffraction (SPring-8).

Fig.2 shows the synchrotron X-ray diffraction photograph of uniaxially drawn (3 times) PVA/MMT nanocomposite taken from the film edge, and schematic of MMT in-plane orientation. By drawing, PVA chains were oriented along the draw direction; which is commonly observed. Beside PVA orientation, MMT layer are found to orient in the direction parallel to the draw direction; which was obvious from the meridional concentration of 060 reflection of MMT. This in-plane stacking of the exfoliated MMT layer prevents the crack propagation during the tensile test, which is considered to result in the increase of the elongation at break of the PVA/MMT nanocomposite.

By adding PVA to the clay aqueous suspension, clay was exfoliated and PVA was intercalated without any organic modifications. Thus, it was revealed that the nanocoposite could be prepared by this simple method. PVA is well known as a biodegradable polymer, and clay used in this study is not organically modified. Accordingly, this composite can be called not only as Nano-Composite, but also as Eco-Composite.

In addition to PVA/MMT composite, we engaged in the preparation of cellulosic nanocomposite. L-lactic acid was *in situ* polymerized in the presence of cellulose nanofiber. This is also new type of Eco-& Nano-composite.

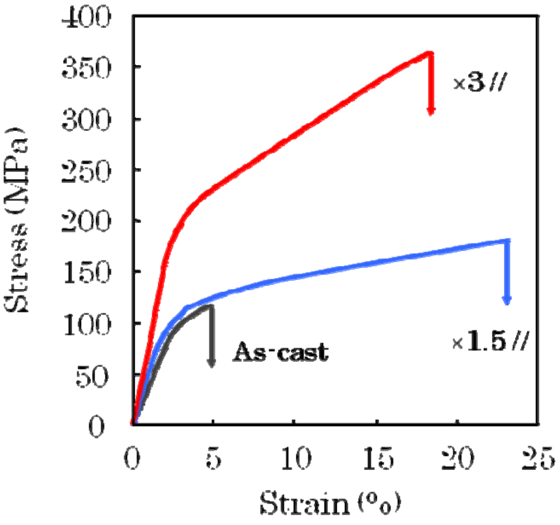

Fig.1 Stress-strain curves of as-cast and uniaxial drawn PVA/MMT nanocomposites drawn at 120℃.

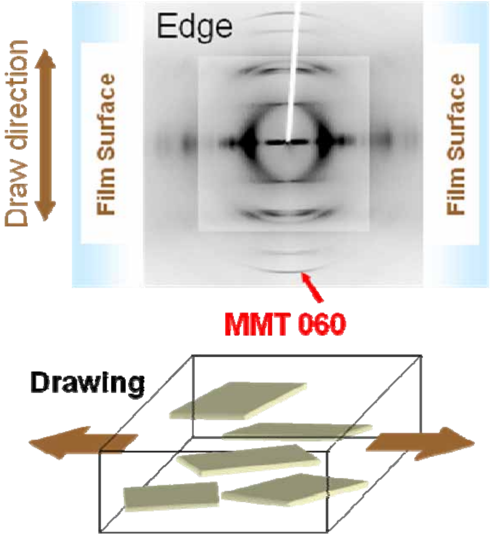

Fig.2 X-ray diffraction photograph of uniaxially drawn (3 times) PVA/MMT nanocomposite taken from film edge, and schematic of MMT in plane orientation.

References

[1] "*Polymer-Clay Nanocomposites*", T. J. Pinnavaia and G. W. Beall eds., John Wiley & Sons, New York (2000).

[2] S.C.Advani, "*Processing and Properties of Nanocomposites*", World Scientific & Imperial College Press, London (2006).

[3] A. Usuki, M. Kawasumi, Y. Kojima, Y. Fukushima, A. Okada, T. Kurauchi, O. Kajimoto, *J. Mater. Res.*, **8** (1993) 1174.

[4] Unitika Ltd., Jpn Patent; Tokkoushou 58-35211.

OP-18

Real-time spectroscopic ellipsometry of silver nanoparticle formation in polymer thin films

T.W.H. Oates
School of Physics,
University of Sydney, 2006,
Australia
E-mail : oates@physics.usyd.edu.au

Monitoring the optical properties and nanoparticle growth in polymer-metal nanoparticle composites, non-destructively and in real time, is highly desirable to be able to control the particle size and distribution during the particle formation. Spectroscopic ellipsometry has been proposed as a powerful method for analysing polymer-nanoparticle composites [1], however very few practical studies have been reported, and none of these have presented dynamic data. This paper will look at using dynamic spectroscopic ellipsometry to study the formation of silver nanoparticles in polymer thin films, which are commonly utilised as substrates in surface enhanced Raman spectroscopy (SERS) [2].

Silver nanoparticle formation in polystyrene and poly(vinyl alcohol) thin films was analyzed in real time by spectroscopic ellipsometry. Polymer films containing a silver precursor were prepared by spin coating to a thickness of less than 100nm. Silver nanoparticle formation was induced by heating the substrate. Spectroscopic ellipsometry was performed *in situ*. A complete spectroscopic scan was recorded every 7 seconds providing real time data of the nanoparticle formation. Further heating of the films evaporated the polymer leaving the particles well dispersed on the substrate surface. Electron microscopy revealed the particle size and morphology (figure 1).

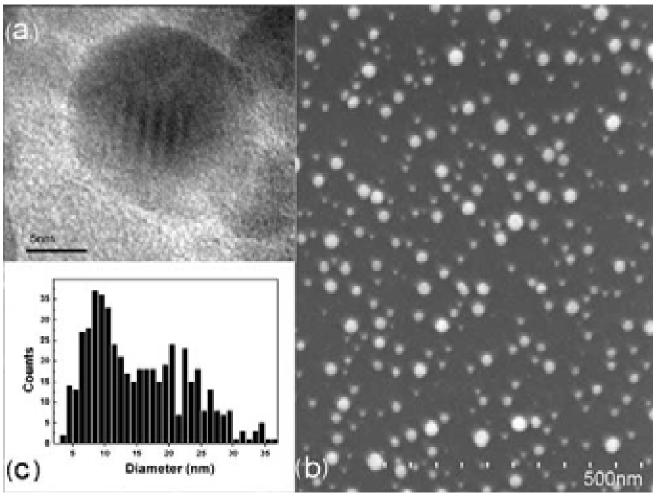

Fig.1 a) TEM of silver nanoparticle in polystyrene. b) SEM of nanoparticles dispersed on substrate surface after evaporation of the polymer c) histogram of particle dimensions

Modeling the ellipsometric data using the Maxwell-Garnett theory (figure 2) shows that the silver content predicted by the model depends on the film thickness. This is conjectured to be due to the strong damping of plasmon resonances in very small particles affecting the model. Modelling the silver particles using the Drude model reveals important information concerning the nucleation and growth of the silver nanoparticles. The size dependence of the free electron relaxation frequency is used to analyse the particle size [3], giving a real time measurement of the particle radius (figure 3).

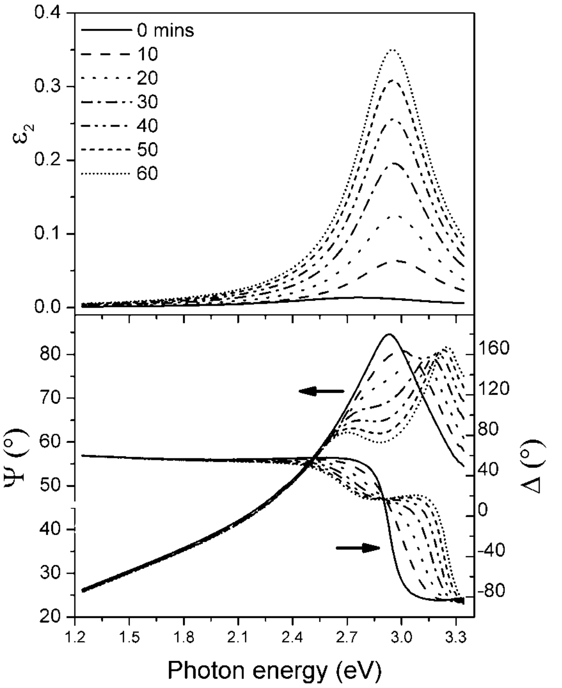

Fig.2 Ellipsometric data during the nanoparticle formation (bottom) and the growing plasmon resonance deduced from the modeling (top).

Evaporation of the polymer matrix is also monitored by real time ellipsometry and the plasmon resonance is observed to shift from 3.0 to 2.2 eV as the particles are liberated from the polymer [4]. The particle density on the surface can be controlled by the silver concentration and the initial polymer thickness. This provides a novel way to control the plasmon resonance frequency and also to disperse nanoparticles on a surface without complicated pretreatment. The exposed particles are easily imaged with scanning electron microscopy, and the particle sizes are compared to the parameters predicted from the Maxwell-Garnett theory.

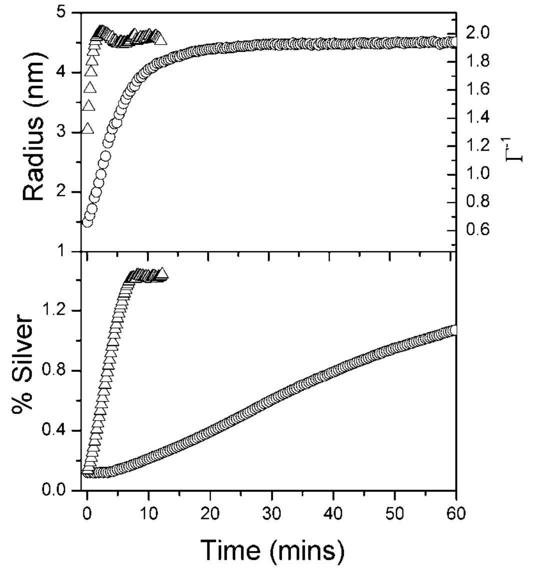

Fig.3 Real time results showing the nanoparticle radius and proportion of metallic silver in the films during heating at 120°C (circles) and 150°C (triangles).

References

[1] U. Riss, *2nd International workshop on Polymer/Metal nanocomposites*; GKSS Forschungszentrum: Geesthacht, Germany, 26-27 September 2005.

[2] D-G Yu et al., Materials Chemistry and Physics **101** 93–98 (2007)

[3] T.W.H. Oates, Applied Physics Letters, **88** 213115 (2006)

[4] T.W.H. Oates, E. Christalle, Journal of Physical Chemistry C, **111**, 182-187 (2007)

Poster Session (PS)

PS-1

Titanyl Phthalocyanine and/or Plasma Polymerized Thiophene and Titania Bilayer Thin Films

M. Drabik1), A. M. Zachary2), Y. Choi2), J. Hanus1), J. Matousek1), O. Polonskyi1), J. Tousek1), J. Touskova1), V. Cimrova1),3), Z. Remes4), D. Slavinska1), H. Biederman1)*, L. Hanley2)

1) Charles University, Faculty of Mathematics and Physics, Department of Macromolecular Physics, V Holesovickach 2, 18000 Prague 8, Czech Republic, Fax.: (+420) 2-2191-2350, E-mail: bieder@kmf.troja.mff.cuni.cz
2) University of Illinois at Chicago, Department of Chemistry, 845 W. Taylor SES 4500 Chicago, IL 60607, USA
3) Institute of Macromolecular Chemistry, Academy of Sciences of the Czech Republic, Heyrovskeho nam. 2, 162 06 Prague 6, Czech Republic
4) Institute of Physics, Academy of Sciences of the Czech Republic, Cukrovarnicka 10, 162 53 Prague 6, Czech Republic

Conducting polymers and their thin films are being extensively studied because of their suitable properties for application in many fields of electrical or electronic engineering, for example as light-emitting devices or thin film transistors in microelectronics and lately as photovoltaic materials.

One class of these organics is phthalocyanines (abbreviated Pc). They are highly stable, economical and easy to handle. Phthalocyanine films have been studied for their possible use in solar cells, field effect transistors and organic light emitting devices (OLEDs). Their structure is highly conjugated with polyaromatic ring that can be bound to a divalent transition metal (MPc) or to hydrogen (H_2Pc). The nature of the central metal atom partly affects photophysical properties of phthalocyanines and is closely related to the charge or the behavior of the photogenerated charge. With an absorbance spectrum that matches the solar spectrum, phthalocyanines are good candidates for e^- donors in organic solar cells.

Various techniques can be utilized for preparation of thin films of conducting polymers. They are either wet (doctor blading, spin coating, etc.) or vacuum methods. Deposition of conducting polymer thin films by means of vacuum technologies can introduce possibilities of further applications. The plasma polymerization as a plasma assisted deposition process is a well-known and efficient method to produce organic thin films and offers good control over the film properties. Films can be deposited over a relatively large area homogeneously and pinhole free. Another possibility is via surface polymerization by ion-assisted deposition (SPIAD) which has been previously demonstrated as an effective method for the production of polythiophene and polyphenylene thin films. This involves simultaneous deposition of polyatomic ions and evaporated neutrals. These studies strongly suggested that SPIAD can be used for polymerization of various types of compounds, especially organic compounds with extended π networks.[1-3] We focus here on studying the electrical and photovoltaic properties of these phthalocyanine films.

To utilize the suitable properties of organic thin films in solar cells, it is convenient to create a donor-acceptor interface where the charge separation occurs.[4] One possible solution is formation of a heterojunction device. It can either be a bilayer heterojunction, a bulk heterojunction or a diffuse bilayer heterojunction. One of the most widely utilized and studied semiconductor materials is titania (TiO_2). Titania is n-type material and its film is proposed to serve as an electron transport layer.

At first, titanyl phthalocyanine (TiOPc) (Fig. 1) thin films were studied. They were prepared using evaporation and surface polymerization by ion-assisted deposition (SPIAD) in an UHV deposition system. These films were characterized by means of ultraviolet and X-ray photoelectron spectroscopy as well as UV/Vis absorption spectroscopy. Valence band and elemental content indicate that phthalocyanine electronic and chemical structures are largely preserved during SPIAD.

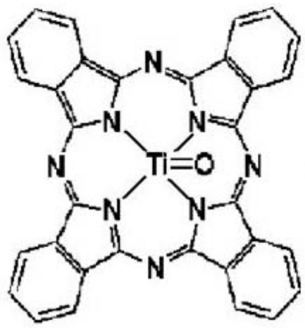

Fig. 1. Structural formula of titanyl phthalocyanine monomer.

In addition, bilayer thin films of titania (TiO_2) and SPIAD TiOPc were prepared as a preliminary version of other nanocomposite thin film systems that will be studied in future. As precedent preparation step, TiO_x/hydrocarbon plasma polymer nanocomposite films (TiO_x/pPP) were prepared by magnetron sputtering of TiO_2 and polypropylene targets as described in our previous study.[5] In this study of the bilayer samples of titania (TiO_2) and SPIAD TiOPc we examined the optical and electrical properties of the composite films. TiO_2 film was deposited by reactive magnetron sputtering of TiO_2 target. The samples of bilayer films were characterized by non-contact photovoltage measurements, I-V characteristics and UV-Vis spectroscopy.

Another promising nanocomposite thin film system is TiO_2 /plasma polymerized thiophene (Fig. 2). We also report here on plasma polymerized thiophene. We prepared thin plasma polymer films from thiophene monomer vapors in a plan parallel plate electrode reactor. A water-cooled magnetron with a carbon target was used as an excitation electrode. Plasma was excited by RF power generator in either continuous wave mode or pulse mode (duty cycles from 2% to 90%). We characterized the samples with respect to their preparation conditions. Thicknesses of the films were measured by a Surfometer and by AFM. The FTIR and XPS techniques were used to gain information on the chemical structure of the films. Ageing and changes in chemical structures of the samples were studied and showed oxidation of the plasma polymer. Basic characteristics of plasma polymerized thiophene and titania bilayer thin film system are given and discussed.

Fig. 2. Structural formula of thiophene monomer.

References

[1] Y. Choi et al., Chem. Mater., 2004, 16, 1924.
[2] S. Tepavcevic et al., Lang., 2004, 20, 8754.
[3] Y. Choi et al., Inter. J. Mass Spectrom. Ion Proces., 2005, 241, 139.
[4] H. Hoppe, N. S. Sariciftci, J. Mater. Res., 2004, 19, 1924.
[5] M. Drabik et al., Plasma Process. Polym., 2007, 4, 654.

Acknowledgements

This work was financed by the grants GAUK 2421/2007 from the Grant Agency of Charles University in Prague, Kontakt 1P04ME754 from the Ministry of Education, Youth and Sports of the Czech Republic and U.S. NSF CHE-0241425.

PS-2

Ni Nanoparticles/DVB Microsphere Composite : Control of Particle Diameter and Interparticle Spacing

Takaaki Tsuruoka1), Satoshi Adachi1), Shingo Ikeda1), Kensuke Akamatsu1), 2), Hidemi Nawafune1), Satoshi Tomita3)

1) Faculty of Science and Engineering, Konan University, 8-9-1 Okamoto, Higashinada, Kobe 658-8501, Japan

2) PRESTO, Japan Science and Technology Agency, Wako, Saitama 351-0198, Japan

3) Graduate School of Materials Science, 8916-5 Takayama, Ikoma, Nara 630-0192, NAIST, Japan

E-mail : akamatsu@center.konan-u.ac.jp

We describe an experimental study involving a novel approach for fabrication of Ni nanoparticles dispersed in divinylbenzene (DVB) microspheres. The process relies on the hydrolysis of DVB microspheres (cross-linked through ester groups) using NaOH aqueous solution to form carboxylic acid groups and incorporation of Ni^{2+} ions by ion exchange reaction followed by heat treatment under hydrogen atmosphere. By controlling the hydrolysis reaction time, we demonstrate systematic control over the amount of Ni^{2+} ions in the sphere, and the size and amount of embedded Ni nanoparticles. More significantly, DVB microsphere size decreased with increasing heat treatment time while the nanoparticle size was almost constant. This was achieved by metal-catalyzed decomposition of surrounding polymer matrices upon heat treatment, leading to a decrease in the spacing among Ni nanoparticles. These results indicate Ni nanoparticle size and interparticle spacing can be independently controlled by changing the experimental conditions. Such the control over the parameters in nanocomposites is an important for potential applications and lead to fundamental understanding of the relationship of the magnetic properties to the composite microstructures.

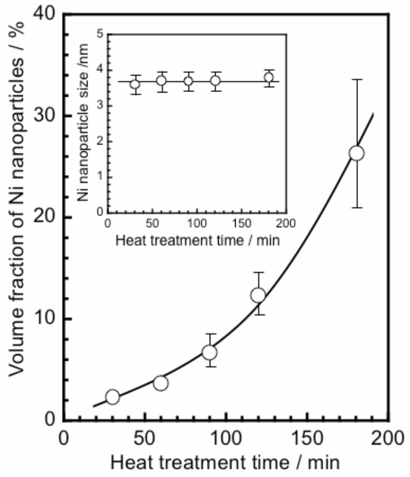

Figure. Effect of heat treatment time on volume fraction of Ni nanoparticles. Inset: Effect of heat treatment time on Ni nanoparticle size.

PS-3

THREE-DIMENSIONAL OPTICAL ARRANGEMENTS OF MAGNETIC SEMICONDUCTOR EUS NANOAGGREGATIONS

Atsushi TANAKA, Tadao SUGIURA[1], Yasuchika HASEGAWA[*], and Tsuyoshi KAWAI[*]

Graduate School of Materials Science, Nara Institute of Science and Technology, 8916-5 Takayama-cho, Ikoma, Nara 630-0192, Japan

[1]Graduate School of Information, Nara Institute of Science and Technology, 8916-5 Takayama-cho, Ikoma, Nara 630-0192, Japan

[*]E-mail address: hasegawa@ms.naist.jp, and tkawai@ms.naist.jp

Introduction

Europium(II)sulfide (EuS) is a magnetic semiconductor having the degenerated 4f orbitals between the conduction band and the valence band [1]. The 4f-5d electronic transition and spin configuration of EuS result in the unique photophysical and magneto-optical properties of EuS [2]. These characteristic properties are strongly dependent on EuS crystal size. The quantum-confinded model predicts that EuS nanocrystals will show enhanced optomagnetic properties including large Faraday and Kerr effects [3]. The three-dimensional (3D) ordering and alignment of functional EuS nanocrystals on the microscale would be desirable for developing future functional materials and devices such as isolators and photomagnetic memories [4]. Here, we report the first demonstration of the manipulation of optomagnetic EuS nanocubes in the aggregated structure using laser trapping techniques.

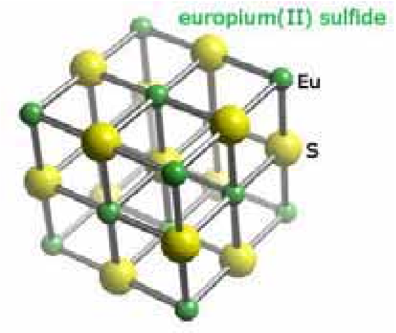

Fig.1 EuS crystal

Experiments and Results

EuS nanocrystals were prepared by the thermal reduction of a single source precursor, tetraphenylphosphonium tetrakis(diethyldithiocarbamete)europium(III) dehydrate $[(PPh_4)^+[Eu(Et_2dtc)_4]^- \cdot 2H_2O]$. First, hexadecylamine was heated to 300 ºC under nitrogen atomosphere, and the single source precursor was quickly injected into the hot hexadecylamine and agitated for 6 h at 300 ºC. The obtained powder was washed by centrifugation for several times with *n*-hexane, and characterized by the X-ray diffraction (XRD) analysis measurement. The transmission electron microscope (TEM) images of EuS nanocrystals are shown in Fig. 2(a). Cubic-shaped nanocrystals with clear lattice fringes were observed, and the electron diffraction pattern had shown good agreement with the isometric EuS lattice. The average size of the EuS nanocrystals was found to be 14 nm. We also observed that the cubic nanocrystals tend to form aggregated structures. To characterize the aggregation of the cubic EuS nanocrystals in the solution phase, we carried out dynamic light scattering measurements in methanol (DLS). The distribution of the particle size exhibited a major contribution of about 328 nm by the DLS measurements(Fig.2 (b)). These results indicate that the cubic-shaped EuS nanocrystals form characteristic self-aggregations in methanol.

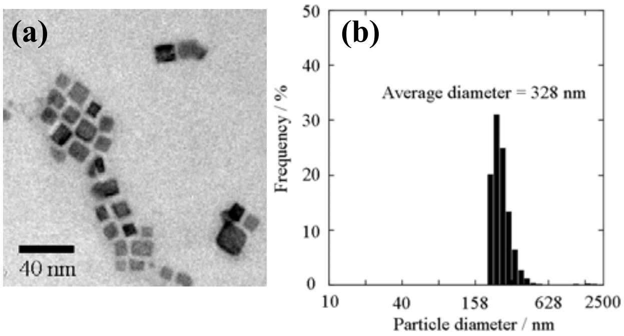

Fig.2 (a) TEM images of EuS nanocrystals, and (b) size Distribution of EuS nanoaggregations using dynamic light scattering method.

The EuS self-aggregation of about 328 nm in diameter is expected to be manipulated by laser trapping, because the refractive index of EuS crystals (n=2.43) is considerably larger than that of surrounding methanol (n=1.33). Here, we demonstrated the 3D arrangements of the EuS nanoaggregations on glass substrates using laser trapping experiment. The CCD image of the 3D arrangements is shown in Fig.3. The assemblies of the EuS nanoaggregations in the cell were successfully patterned as “E” and “T” on the glass substrate. These results indicate that EuS aggregations in methanol can be independently manipulated using laser trapping techniques.

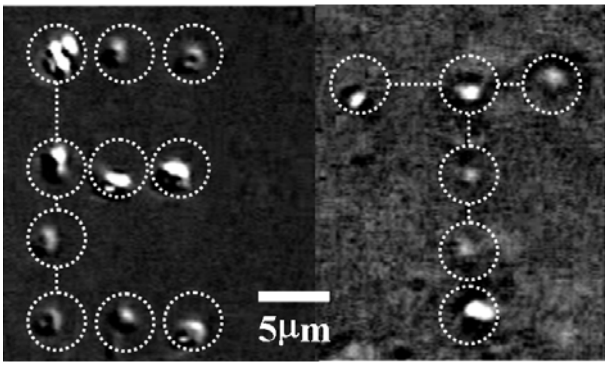

Fig.3 CCD images of three-dimensional arrangements of EuS aggregations by laser trapping.

Conclusion

3D optical arrangements of magnetic semiconductor EuS nanoaggregations in organic media were successfully demonstrated for the first time. The 3D arrangements of EuS nanoaggregations having optomagnetic properties are expected to open up pioneering fields in microscaled magnetics, optics, and materials science.

References

[1] T. Kasuya, and A. Yanase: Rev. Mod. Phys. **40** (1968) 684.

[2] C. Muller, H. Lippitz, J. J. Paggel, and P. Fumagalli: J. Appl. Phys. **95** (2004) 7172.

[3] K. Tanaka, N. Tatehata, K. Fujita, and K. Hirao: J. Appl. Phys. **89** (2001) 2213.

[4] Y. Hasegawa, S. Thongchant, Y. Wada, H. Tanaka, T. Kawai, T. Sakata, H. Mori, and S. Yanagida: Angew. Chem., Int. Ed. **41** (2002) 2073.

PS-4

Molecularly Imprinted Polymer Nanocomposite for Highly Sensitive Surface Plasmon Resonance (SPR) Detection of Herbicides

Megumi Takayose1), Jun Matsui1,2), Kensuke Akamatsu1,2), Hidemi Nawafune1,2), Katsuyuki Tamaki1), Naoki Sugimoto1,2)

1) Faculty of Science and Engineering, Konan University, 8-9-1 Okamoto, Higashinada-ku, Kobe 658-8501, Japan

2) Frontier Institute for Biomolecular Engineering Research (FIBER), Konan University, 8-9-1 Okamoto, Higashinada-ku, Kobe 658-8501, Japan

E-mail: sugimoto@konan-u.ac.jp

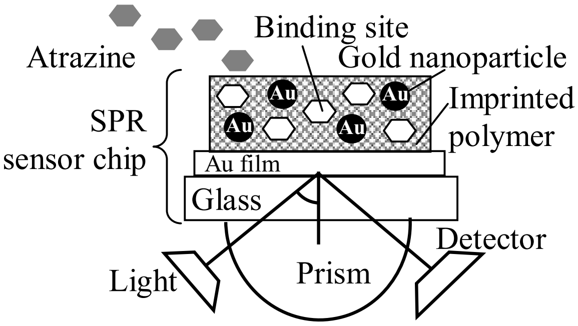

Figure 1. Schematic illustration of an SPR sensor chip covered with gold nanoparticle-immobilized imprinted-polymer.

In the past decade, various technologies for detection and measurement of environmental pollutants such as endocrine disturbing chemicals have been developed. Particularly, biosensors have attracted increasing attention because they are potentially sensitive and selective to specific analyte molecules. A surface plasmon resonance (SPR) device is one of the most promising transducer of biosensors because high-throughput, imaging, and dawn-sizing technologies are developed. However, an SPR sensor has a shortcoming that it is not sensitive, in principle, towards a low molecular-weight analyte. Therefore, tactics for devising sensor chips sensitive for such analytes have been required.

For sensitive detection of a small molecule, a sensor chip is required to 1) show high affinity for a small molecule and 2) possess enhanced electromagnetic field for magnify a change in polarity derived from an analyte-binding event. On this basis, in this study, we develop a sensor chip using a molecularly imprinted polymer and gold nanoparticles (Figure 1). It has been reported that a molecularly imprinted polymer can be prepared by complexation of a template molecule and functional monomers, cross-linking the complexes, and removing the template molecule from the resultant network polymer. The imprinted polymer is expected to possess a template-selective binding site and therefore work as molecular recognition elements, thus making the resultant sensor chip to be selective. The sensor chip is also expected to be sensitive due to coupling phenomena of gold nanoparticles in the imprinted polymer and the gold thin film on a glass substrate.

An herbicide atrazine, known as an endocrine disturbing chemical, was used as a proof-of-principle target. Preparation of a sensor chip was conducted as following; surfaces of two gold-sputtered glass plates were modified with a vinyl group and alkyl group, respectively. A monomer mixture, consisting of methacrylic acid, ethylene dimethacrylate, 2,2’-azobisisobutyronitrile, atrazine (a template molecule), gold nanoparticles modified with 11-mercaptoundecanoic acid and DMF, was sandwiched between the two glass plates and heated at 60°C for 4 h. The resultant plate covered with the imprinted polymer incorporating gold nanoparticles (IP17.4) was used for SPR measurements. Acetonitrile was used as a carrier at a flow late of 15 μL min^{-1} at 24°C.

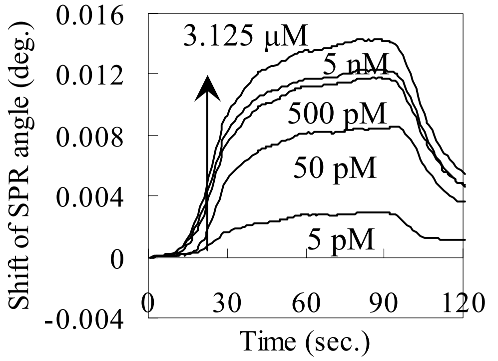

Figure 2. Sensorgrams of IP17.4 upon injection of atrazine-acetonitrile solution. The sample volume was 20 μL.

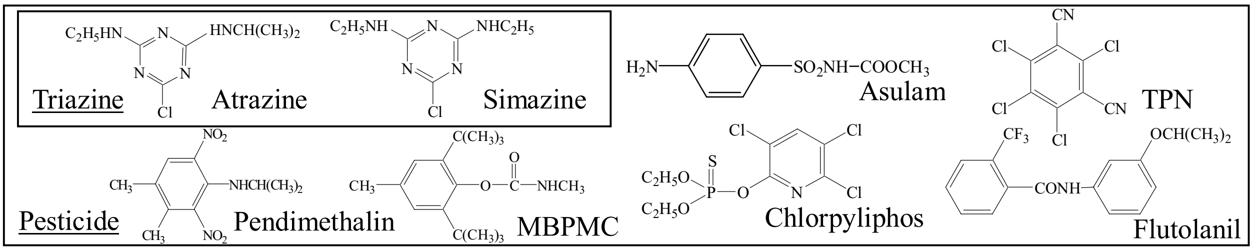

Figure 3. Structure of agrochemicals used for SPR measurements.

Response (shift in the SPR angle) to atrazine in the case of IP17.4 is shown in Figure 2. A larger shift in SPR angle was obtained in accordance with an increase in the atrazine concentration, suggesting that IP17.4 is useful to determine the atrazine concentration with a detection limit as approximately 5 pM. Selectivity was investigated by examining other agrochemicals shown in Figure 3; atrazine resulted in a larger shift than the reference agrochemicals including a structurally similar triazine herbicide, simazine. In the case of using a sensor chip covered with a non-imprinted polymer, no selectivity towards atrazine was observed. These results suggested that the combinational use of gold nanoparticles and the molecularly imprinted polymer was effective for developing an SPR sensor chip that is sensitive and selective for a low-molecular weight species.

References

[1] J. Matsui, K. Akamatsu, N. Hara, D. Miyoshi, H. Nawafune, K. Tamaki, and N. Sugimoto, *Anal. Chem.*, **77**, 4282-4285 (2005).

[2] J. Matsui, K. Akamatsu, S. Nishiguchi, D. Miyoshi, H. Nawafune, K. Tamaki, and N. Sugimoto, *Anal. Chem.,* **76**, 1310-1315 (2004).

PS-5

Synthesis and spectroscopic studies of dendrimer-Au hybrid nanoclusters

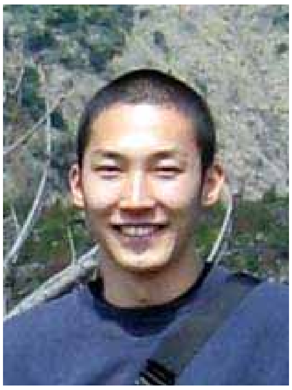

Yoshiaki Murase[1)], Takanobu Kitagawa[1)], Akinori Tanaka[1)], Hidehiro Yasuda[1)], Yuichi Negishi[2)], Tatsuya Tsukuda[2)]

[1)] Department of Mechanical Engineering, Kobe University, Nada-ku, Kobe 657-8501, Japan

[2)] Department of Materials Molecular Science, Institute for Molecular Science, Myodaiji, Okazaki 444-8585, Japan

E-mail : 062t411n@stu.kobe-u.ac.jp

Metals exhibit a particularly wide range of material behavior along the bulk to atom transition. Usually occurring at the nanoscale, material properties drastically changes as their sizes approach their characteristic length scale. Such quantum confinement effects often yield nanostructured materials with greatly improved and potentially controllable properties. These physical properties of nanoclusters are also strongly dependent on their size. Therefore, in order to investigate the intrinsic size-dependent properties of nanocluster systems, it is necessary to synthesize the monodispersed samples. In this work, we have attempted to synthesize the monodispersed Au nanoclusters using a dendrimer templating approach, and have performed the various spectroscopic studies in order to investigate their optical properties and electronic structures. Dendrimer is a group of highly branched, three dimensional, synthetic macromolecules. Since the dendrimer has a cavity inside this macromolecular structure, the dendrimer is used as a template to stabilize the nanocluster against aggregation, to prevent precipitation of metal nanocluster, and to define the nanocluster size.

We have prepared the dendrimer-Au hybrid nanoclusters by the method developed by Zheng *et al.* [1] In this work,

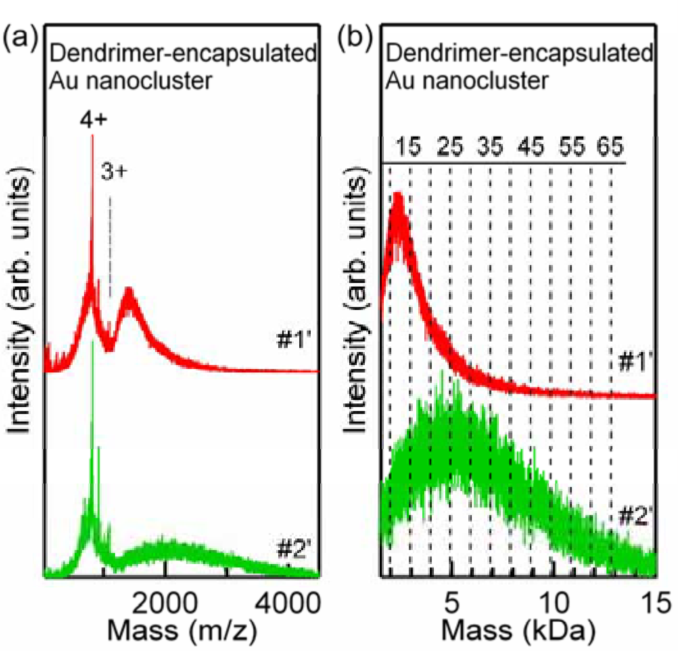

Figure 1. ESI mass spectra of G2-OH dendrimer encapsulated Au nanocluster.

we have used the second generation OH-terminated (G2-OH) poly(amidoamine) (PAMAM) dendrimer. An aqueous solution of G2-OH PAMAM dendrimers and $HAuCl_4$ were mixed with a distilled solution, and then gold ions were reduced by $NaBH_4$. Reduced gold atoms aggregate to form the nanoclusters. Solutions were subsequently purified through the size-selective ultrafiltration treatments. From the transmission electron micrographs and electrospray ionization (ESI) mass spectroscopies, the present ultrafiltration treatments allows us to divide among Au nanoparticles stabilized outside the dendrimer with diameter larger than 2 nm and the relatively smaller ones encapsulated inside cavity of dendrimer with diameter less than 1 nm. Figure 1 (a) shows the experimental ESI mass spectra of the dendrimer-encapsulated Au nanoclusters prepared in this work as a function of m/z (mass divided by charge), and the mass spectra in Fig. 1 (b) are reproduced from the most intense peaks in the corresponding ESI mass spectra in Fig. 1 (a) as a function of mass. As shown in Fig. 1 (b), it is found that the mean mass numbers of the present dendrimer-Au nanocluster samples are Au_{13} and Au_{25}, however, the present samples were accompanied with the finite size distributions. While the extinction spectra of relatively larger Au nanoparticles (stabilized outside the dendrimer) with diameter larger than 2 nm show the distinct Mie plasmon resonance, the relatively smaller dendrimer-encapsulated Au nanoclusters (Au_{13} and Au_{25} nanoclusters) show no Mie plasmon resonance. This indicates that the electronic structures of the present dendrimer-encapsulated Au_{13} and Au_{25} nanoclusters change from the metallic states to the non-metallic ones due to the quantum confinement effect. In addition, we have measured the photoluminescence spectra of the present dendrimer-encapsulated Au_{13} and Au_{25} nanoclusters. We have observed the highly blue photoluminescence from the both dendrimer-encapsulated Au nanoclusters as reported in the literature [1, 2]. Zheng *et al.* have concluded that this blue photoluminescence originates from the quantized electronic transition [1, 2]. However, G2-OH PAMAM dendrimer used in this work as a template also exhibits the highly blue photoluminescence quite similar to those of the present dendimer-encapsulated Au nanoclusters. Therefore, it is considered that that G2-OH PAMAM dendrimer using as a template play an important role in the present photoluminescences from the dendrimer-encapsulated Au nanoclusters. From these results, we discuss the detailed optical properties and electronic structures of the dendrimer-Au hybrid nanocluster systems.

References

[1] J. Zheng, C. Zhang, and R. M. Dickson, Phys. Rev. Lett. **93**, 077402 (2004).

[2] J. Zheng, J. T. Petty, and R. M. Dickson, J. Am. Chem. Soc. **125**, 7780 (2003).

PS-6

Molecular Manipulation at Small Metallic Gate

Hideki Nabika, Baku Takimoto, Masahiro Oowada, Naozumi Iijima, Kei Murakoshi
Graduate School of Science, Hokkaido University,
N10W8, Kita, Sapporo, Hokkaido 060-0180, Japan
E-mail : nabika@sci.hokudai.ac.jp

Molecular manipulation in confined space is an important issue for the developments of advanced ultra-small fluidic devices. Although several intriguing systems have been proposed so far, most approaches are based on the traditional electrophoresis techinique.[1] The fact imposes severe restriction that the molecules that could be manipulated are strictly limited into the charged ones. On the other hands, we have recently reported novel molecular separation system that is able to working without any external bias such as electric field.[2] In our system, directional molecular motion was caused by self-spreading nature of lipid bilayer. By introducing small gate with the width less than a few tens nanometers on the spreading substrate, we have found that the molecule doped in the spreading bilayer was gradually separated from the spreading edge during the spreading through the gates. The observed molecular separation was attributed to local structural change of the spreading bilayer at the gate region. Since the solubility of doped molecule is occasionally reduced by the bilayer structural change, penetration ability of the doped molecule into the gate region was thought to be lowered due to the structural change. Thus, the structural control of the spreading bilayer is a key factor that governs the separation efficiency. In the present study, we have examined the effect of gate width and the addition of cholesterol on the molecular separation efficiency. Cholesterol is known to induce drastic phase transition of the bilayer from liquid disordered to liquid ordered phases.

Egg-PC (99%, Sigma-Aldrich), TR-DHPE (Molecular Probes) and cholesterol (Wako) were used without further purification. Spreading of the lipid membrane was conducted according to a previously reported procedure.[3] The spreading behavior was monitored *in-situ* by epi-fluorescence microscopy in 100 mM Na_2SO_4 solution. The periodic array of Au gate channel was fabricated on cover glass substrates using electron beam lithography (ELS-7700H, Elionix Co., Ltd Japan). The gate width was tunes between 500 nm and 75 nm. Typical AFM image of the gate patterns were shown in Fig. 1.

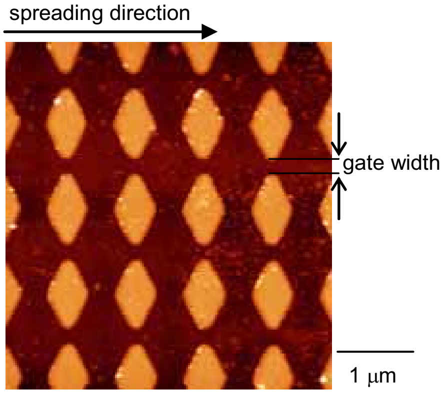

Figure 1. AFM image of the periodic array of gate. The gate width in the image was 200 nm.

First, the effect of cholesterol addition on the self-spreading dynamics was examined. The results (Fig. 2) clearly demonstrated that the cholesterol addition lowered the self-spreading velocity due to the reduction in the bilayer fluidity. Although any domain structure was observed under epi-fluorescence microscope, tiny ordered domain of cholesterol molecules, presumably less than 10 nm, were dissolved in the spreading bilayer. With the presence of gates and decreasing the gate width, we have observed decrease in the spreading dynamics, and also increment in the molecular separation efficiency. The result implies that the narrower gate induced more significant structural deformation at the gate region. Furthermore, the addition of cholesterol enhances both changes. During passing through the gate, imposed stress by the narrow gate would induce phase transition from loosely packed disordered to highly ordered phases. This transition lowers both the bilayer fluidity and the penetration probability of TR-DHPE into the gate region. Our results demonstrate that structural control at the gate region, by optimizing the bilayer composition and the gate structure, will be a critical parameter for our molecular separation system.

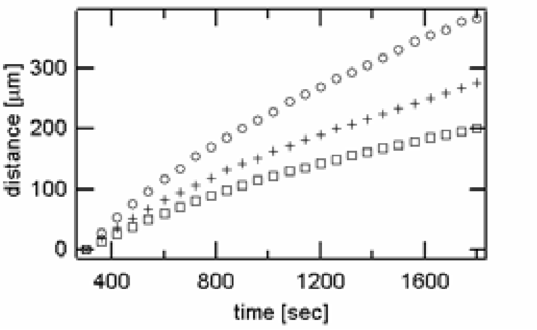

Figure 2. Spreading distances of egg-PC lipid bilayer as a function of time. Cholesterol concentrations were (○) 0 %, (+) 10 % and (□) 20 %.

References:

[1] (a) J. Han, H. G. Craighead, *Science* **288**, 1026 (2000). (b) A. van Oudenaarden, S. G. Boxer, *Science* **285**, 1046 (1999).

[2] H. Nabika, A. Sasaki, B. Takimoto, Y. Sawai, S. He, K. Murakoshi, *J. Am. Chem. Soc.*, **127**, 16786 (2005).

[3] (a) H. Nabika, A. Fukasawa, K. Murakoshi, *Langmuir* **22**, 10927 (2006). (b) J. Nissen, S. Gritsch, G. Wiegand, J. O. Radler, *Eur. Phys. J. B* **10**, 335 (1999).

PS-7

High dispersion of gold nanoparticles in the porous resin bead supported by amphiphilic vinyl-malate copolymer

Waki Yukita1), Yukiko Takahashi1), Maya Chatterjee1), Toshishige Suzuki1)

1) Research Center for Compact Chemical Process,
National Institute for Advanced Industrial Science and Technology (AIST)
4-2-1, Nigatake, Miyagino-ku, Sendai, 983-8551, Japan

E-mail : yukiko-takahashi@aist.go.jp

Highly dispersed arrangement of metal nanoparticles on solid substrate is critically important for practical application to electronic and optic devices, sensors and catalysts due to enhance the functions of individual nanoparticles. Particularly, anchoring of catalytically active nanoparticles onto solid substrates provides advantages of easy recovery and recycling of the catalysts. In the supported catalyst, it is desirable that each metal particle does not aggregate each other and has the uniform size and shape. Polymers having metal binding site have been successfully applied as the stabilizer in the preparation of metal nanoparticles.[1]

To achieve this purpose we have designed the polymer composite material in which amphiphilic copolymers composed of maleic acid and C_{18} vinyl monomer unit holding metal nanoparticles are encapsulated in the pores of porous resin beads (**Scheme 1**). We have described the successful synthesis of highly stabilized and highly dispersed Au nanoparticles encapsulated in the pores of cross-linked polyacrylate resin (HP2MG) and cross-linked polystyrene resin (XAD4) without aggregation of particles. The above mentioned synthesis was based on two notable features: 1) linear copolymer can stabilize Au nanoparticles with multipoint coordination by flexibly changing the molecular shape, 2) hydrophobic alkyl chains oriented outward act as the anchor to pore of beads by hydrophobic interactions. Au nanoparticle was applied to the catalytic hydrogenation of cinnamaldehyde in supercritical carbon dioxide ($scCO_2$) to elucidate the size effect of Au nanoparticle on the conversion and selectivity of the reaction.

An amphiphilic copolymer composed of maleic anhydride and alkyl (C_{18}) vinyl monomer was encapsulated into porous beads HP2MG and XAD4. Because maleic anhydride moiety can be modified to various functional groups, *e.g.*, carboxylic acid, hydroxamic acid and ethylenediamine by simple treatment, the resin-polymer composite can be applied to stable loading of various metal nanoparticles. Citric acid has been used extensively to synthesize and stabilize Au nanoparticles. Maleic acid moiety in the linear polymer produced by simple hydrolysis of maleic anhydride acts as the stabilizer for Au nanoparticle in analogy with citric acid and the reaction was followed by IR measurement. The linear polymer was confirmed to accommodates predominantly in the 20-100 μm

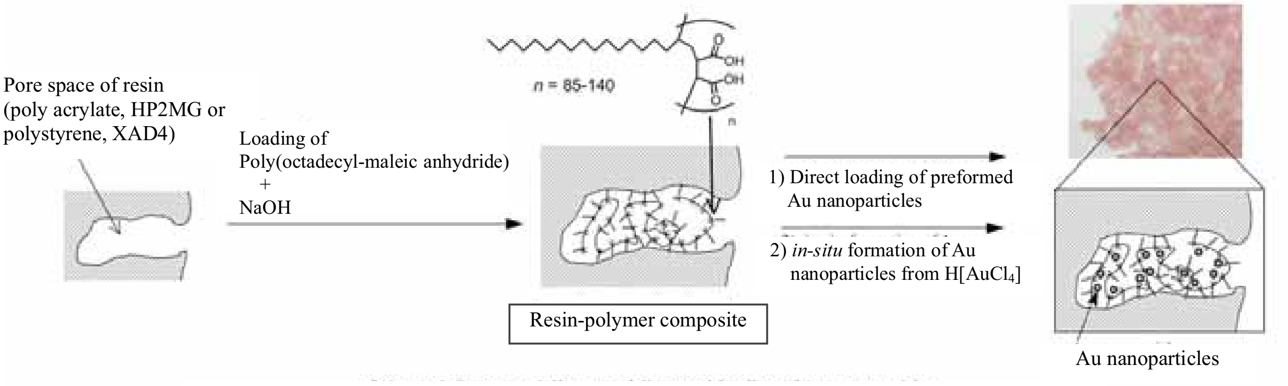

Scheme 1 Conceptual diagram of dispersed loading of Au nanoparticles

from the resin surface by SEM-EDX measurements of Cu(II) probe. Preformed Au nanoparticles of known size (2-50 nm) were substantially loaded in the resin-polymer composite without particle aggregation (**Fig. 1a**). Similarly, retention of Au nanoparticles occurred by treated only with vacant resin, but resulted in serious aggregation of particles (**Fig. 1b**). Presence of C_{18} alkyl chain in the linear polymer is indispensable to act as spacing group that prevents mutual aggregation of particles. Additionally, *in-situ* sysnthesis of Au nanoparticles from aqueous $H[AuCl_4]$ was successful with average diameter of less than 10 nm by using the resin-polymer composite without particle aggregation. Noteworthy, Au nanoparticles were not formed in the absence of linear polymer, either in the case of HP2MG or XAD4. Leaching of Au into aqueous solution practically did not observed by shaking the Au nanoparticle loaded resin beads in water for 1 week. The amounts of preformed and *in-situ* synthesized Au are 35-88 μg and 1.4 mg in 1g of resin-linear polymer composite, respectively.

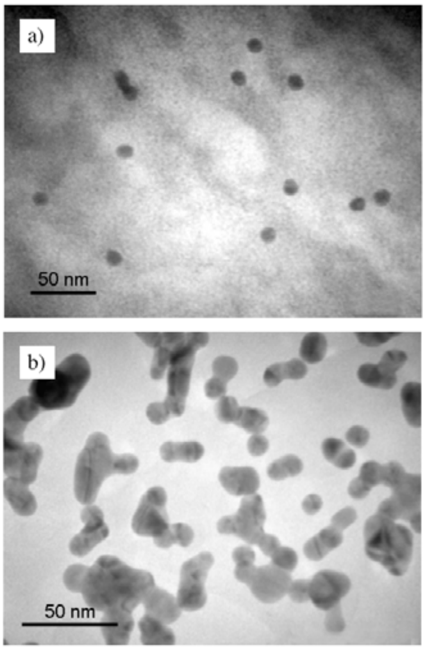

Fig.1 Typical TEM images of preformed Au nanoparticles (15 nm) retained on HP2MG- linear polymer composite(a) and XAD4 in the absence of the linear polymer (b).

The catalytic activity of the Au nanoparticle loaded resin beads was examined for the selective hydrogenation of *trans*-cinnamyl aldehyde in supercritical carbon dioxide at 50°C. Cinnamaldehyde is an unsaturated aldehyde which contains C=O and C=C bonds susceptible for hydrogenation (**Scheme 2**). It is well known that the hydrogenation of C=O is more difficult because both kinetics and thermodynamics favor the hydrogenation of C=C. The blank sample did not show any catalytic activity. Notably, apparent size effect of Au was observed in the selectivity, *i.e.*, particle size smaller than 10 nm preferentially produced cinnamyl alcohol (P1) in a *ca.* 90% yield. Increase in the particle size from 15 to 50 nm resulted in decrease of P1 selectivity along with the increased formation of hydocynnamyl aldehyde (P2). The hydrogenation of cinnamaldehyde is structure sensitive and it is favored on smaller particle of catalysis. Additionally, in $scCO_2$ medium the smaller particle reduces the interparticle diffusion, which is related to the viscosity of the medium and attribute to the high selectivity.[2] The *in-situ* formed Au nanoparticles in HP2MG-linear polymer composite gave comparable selectivity of P1 and P2, on the other hand, Au in XAD4-linear polymer composite gave P2 predominantly, although the particle sizes are less than 10 nm. That is presumably because the size distributions are not sharp (RSD 22-24%) and large size particles contributed to the formation of P2.

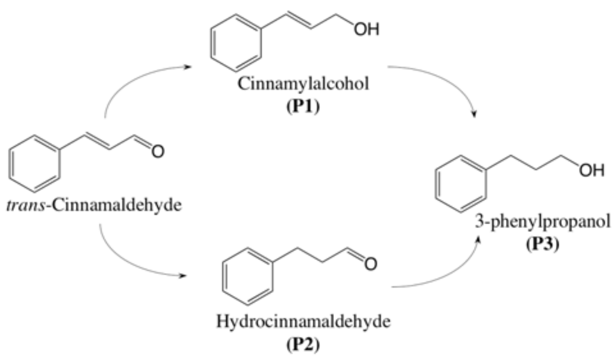

Scheme 2 Possible reaction pathway of cinnamaldehyde hydrogenation in supercritical carbon dioxide.

References

[1] I. Hussain, M. Brust, A. J. Papworth, A. I. Cooper, *Langmuir* **2003,** *19,* 4831; B. G. Ershov, *J. Phys. Chem., B* **1998**, *102*, 10663; H. Hirai, H. Chawanya, N. Toshima, *Reactive Polymers* **1985,** *3*, 127. R. C. Doty, T. R. Tshikhudo, M. Brust, D. G. Fernig, *Chem. Mater.* **2005**, 17, 4630.

[2] O. Krocher, R. A. Koppel, A. Baiker, *J. Mol. Cat. A* **1999**, *140*, 185.

PS-8

Formation and Dispersion Process of Silver Nanopaticles into Glass by Heat Treatment

Yusuke TAKAMURA and Shigehito DEKI
Department of Chemical Science & Engineering, graduate school of Engineering, Kobe university 1-1 Rokkodai, Nada, Kobe 657-8501 Japan
E-mail : takamura@cx2.scitec.kobe-u.ac.jp ,

Introduction

In recent years, metallic nanoparticles doped dielectric materials such as glasses or polymers have attracted much attention due to their potential application in several fields. The properties of these materials are highly dependent on the size, shape and distribution of the nanoparticles. Therefore, the precise control of size and distribution is required. In addition, simple preparation process is necessary for practical application. In this study, we report on preparation of Ag nanoparticles doped glass by using the simple method and also discuss the mechanism of Ag nanoparticle formation in glass.

Experimental

Commercial soda lime glass was used. Metallic Ag was vacuum-evaporated on to the glass. The thickness of deposited Ag was 100 nm. After the vacuum evaporation was completed, the Ag evaporated glass was heat treated at various temperatures for 1 h in air. After heat treatment, samples were washed by HNO_3 to remove Ag remained on the glass surface. Samples were characterized by means of UV-visible (UV-vis) absorption spectroscopy, transmission electron microscopy (TEM), selected area electron diffraction (SAED), X-ray photoelectron spectroscopy (XPS) and Induced coupled plasma-atomic emission spectrometry (ICP-AES).

Results and discussion

The cross-sectional TEM image and SAED pattern of the sample heat treated at 450°C was shown in Fig. 1. Average particle size was about 9.6 nm and these particles were characterized as metallic Ag from SAED. These data suggested that evaporated Ag dispersed into glass and deposited as nanoparticles by heat treatment.

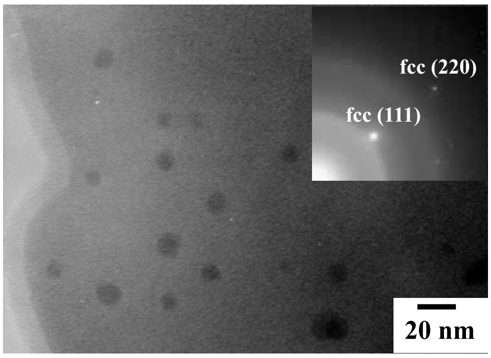

Fig. 1 TEM image and SAED image of Ag evaporated glass heat treated at 450°C.

Optical absorption spectra of samples heat treated at various temperatures were shown in Fig. 2. The absorption bands due to surface plasmon resonance of Ag nanoparticles were observed at around 410 nm. The absorption intensity, indicates the amount of Ag nanopaticles in glass, increased with increasing of heat treatment temperature, and especially increased drastically above 450°C. The glass transition temperature (T_g) of soda lime glass used in this study was 442 °C from DSC analysis. These results suggested that the formation of Ag nanoparticle was accelerated above T_g. This might be explained as follows: The glass network becomes looser above T_g, therefore, the diffusion rate of Ag was enhanced. As a result, Ag nanoparticles deposited in glass increased.

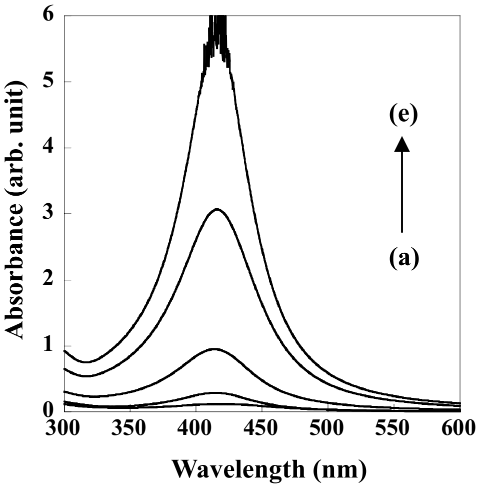

Fig. 2 Optical absorption spectra of Ag evaporated glass heat treated at various temperatures from (a) 350°C to (e) 550°C for 1 h.

PS-9

Preparation of Transition Metal Nanoparticles / Polymer Composite Thin films by Relaxative Auto-Dispersion Method

Yuichirou Morimoto and Shigehito Deki
Department of Chemical Science and Engineering, Faculty of Engineering
Kobe University, 1-1, Rokkodai-cho, Nada-ku, Kobe657-8501, Japan.
E-mail : morimoto@cx2.scitec.kobe-u.ac.jp,

Introduction

Nanoparticulated composites of transition metal are of considerable interest because they have different properties from bulk metal, e.g., optical, electronic and magnetic properties and Such composites are expected a novel functionality material. Since the property of nanoparticle depend on the particle size and size distribution, investigation regarding method of preparing such composite is important. we have previously studied and reported a novel process to prepare metal nanoparticle / polymer composite by a thermal relaxation technique. In this study, we prepared two kinds of metal nanoparticle / polymer composite thin films. The first is Fe-Ni metal oxide nanoparticle / Nylon11 composite thin films, the other is Ni and Co metal nanoparticle / Nylon11 composite thin films by Relaxative Auto-Dispersion method.

Experimental

1: Preparation of Fe-Ni oxide nanoparticles / Nylon11 composite thin films

Nylon11 thin film was prepared by vacuum vapor deposition method and the thickness was 100 nm. The Fe-Ni oxide nanoparticles were prepared by co-evaporation technique onto the nylon 11 film. the ratio of Fe thickness / Ni thickness was 2 : 1, 1 : 1 and 1 : 2 and total thickness was 6 nm. After the deposition, the films were annealed at 100°C and 150°C in an air atmosphere. The samples were characterized by transition electron microscopy (TEM), selected area electron diffraction (SAED), and X-ray photoelectron spectroscopy (XPS).

2: Preparation of Ni and Co metal nanoparticles / Nylon11 composite thin films

Nylon11 thin film were prepared by vacuum vapor deposition method and the thickness was 50 nm. The Ni and Co metal were vapor deposited on their polymer films and the thickness was 2 nm. After the deposition, the films were annealed at 200°C at a pressure of 2.0×10^{-5} Torr. The samples were characterized by TEM, SAED, XPS.

Results and discussion

1. Fe-Ni oxide nanoparticle / Nylon11 composite thin films

From TEM observation, uniformly nanoparticles were observed by samples. Fig. 1 shows Intensity distribution curve taken from SAED patterns of samples. the sample of Fe / Ni = 1 peak conformed $NiFe_2O_4$. As the Ni content increases, these peaks are found to shift towards from Fe single component sample peak to that of Ni single component, these shifts indicate a change of the crystal structure. Depth profile by XPS indicate that Fe-Ni oxide nanoparticles are dispersed in Nylon11 thin film.

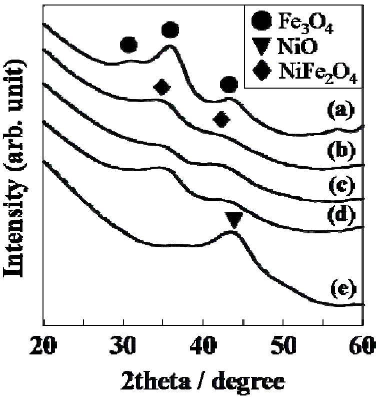

Fig. 1 SAED patterns of nanoparticles dispersed in Nylon11 films after heat treatment at 100°C for 10 min.; (a) Fe, (b) Fe : Ni = 2 : 1, (c) 1 : 1, (d) 1 : 2 and (e) Ni.

2. Ni and Co metal nanoparticles / Nylon11 composite thin films

From TEM observation, Ni samples were observed uniformly nanoparticles, but Co sample was observed polydispersed nanoparticles. Fig. 2 shows intensity distribution curve taken from SAED patterns of samples, and indicate that Ni and Co samples are correspond to metal of each other. By XPS analysis, near-surface nanoparticles on Ni sample were metal state, those of Co sample were metal and oxide mixed states. Depth profile by XPS indicate that Ni and Co metal nanoparticles are dispersed in Nylon11 thin film.

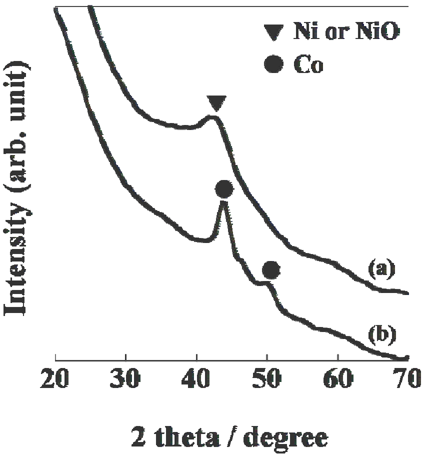

Fig. 1 SAED patterns of Ni and Coi nanoparticles dispersed in Nylon11 films after heat treatment at 150°C for 30 min.; (a) Ni and (b) Co.

PS-10

Synthesis of Pt / PPy on Carbon Composite and Electrochemical Properties for PEFC

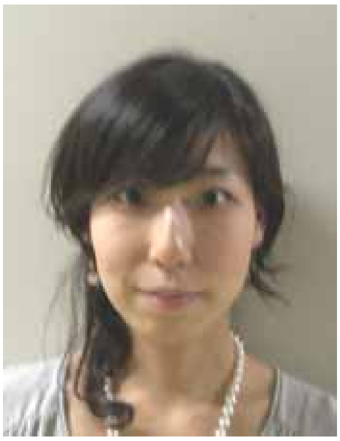

Masako OGA1), Minoru MIZUHATA1), Shigehito DEKI1)
1) Department of Chemical Science and Engineering,
Graduate School of Engineering, Kobe University,
1-1 Rokkodai-cho, Nada, Kobe, 657-8501 Japan
E-mail : oga@cx2.scitec,kobe-u.ac.jp

Polymer electrolyte fuel cell (PEFC) is an attractive energy source in terms of environment. However, it has some problems in operation, such as dissolution and redeposition of platinum used as a catalyst.[1] Polypyrrole (PPy) is one of representative conductive polymers and a lot of reports has been released for the practical use of cell materials using it. We suggested one-step synthesis of Pt / PPy composite through simultaneous reactions of reduction of platinum ion and oxidation of pyrrole monomer.[2] Applying this previous synthesis method, we propose the new electrocatalyst, Pt / PPy on carbon composite. PPy plays a role of blocking layer for suppressing dissolution of Pt.

Vulcan XC-72R carbon was oxidized by immersing in KMnO$_4$ and HNO$_3$ aqueous solution at 343 K for 4 hours. After washing and filtrating for removing extra KMnO$_4$, carbon was stirred in 4 M HCl for 17 hours and modified with carboxylic group. Pt(NH$_3$)$_4$(OH)$_2$ was used as platinum source and ion-exchange occurred between proton of carboxylic group and platinum ion.[3] When pyrrole monomer was applied to carbon dissolved solution, oxidative polymerization of pyrrole got start and Pt / PPy on carbon composite was synthesized. To confirm the durability of Pt / PPy on carbon, multiple sweep of cyclic voltammetry was used and changes of structure during CV were observed by high-resolution transmission electron microscope.

The cyclic voltammogram showed that oxygen reduction reaction occurred about 0.2 V vs. Ag/AgCl when Pt / PPy on carbon composite was used as working electrode. The durability of composite was checked with 10000 cycles of CV, between -0.2 V to

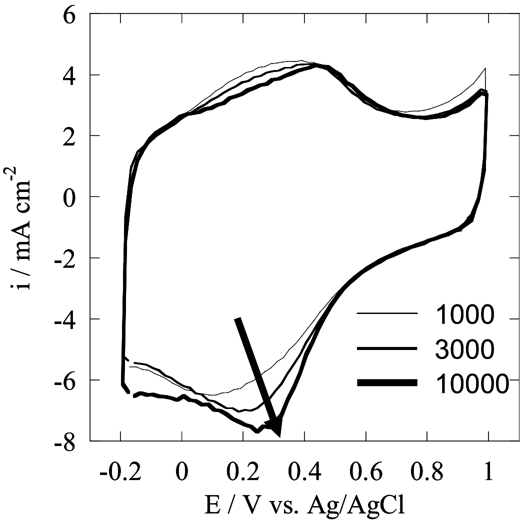

Fig.1. The cyclic voltammogram of Pt / PPy on carbon composite in 0.5 M H$_2$SO$_4$.

1.0 V vs. Ag/AgCl., because practical use of PEFC involves a lot of potential changes under operation. The shape of voltammograms did not show obvious changes and decrease of catalytic activity during multiple sweeps. We observed the transformation of catalyst particles during endurance test, and particles with several nanometers after synthesis increased in size about 10 nm. We also prepared platinum on carbon (Pt / C) electrode and compared the performance with Pt / PPy on carbon. The area of peak for hydrogen adsorption and desorption got smaller after multiple sweeps for Pt / C, in addition, the significant change of platinum particles size was observed.

The increase of catalyst particles size would derive from the dissolution and redeposition process during CV test, and these results indicated that PPy is a useful layer to suppress the deterioration of electrocatalyst.

References

[1] A. Taniguchi et al., *J. Power Sources,* **130**, 42 (2004)

[2] S. Deki et al., *Electrochemistry*, **72,** 415, (2004)

[3] K. Amine et al., *J. Chem. Soc. Faraday Trans*., **91,** 4451, (1995)

PS-11

Cancelled (pp.56-61)

PS-12

Femtosecond time-resolved two-photon photoemission study of dodecanethiolate-passivated Ag nanoparticles

Masaki Imamura, Atsushi Matsumoto, Hisakazu Arita, Shuji Fujimasa, Akinori Tanaka, Hidehiro Yasuda
Department of Mechanical Engineering, Kobe University, Nada-ku, Kobe 657-8501, Japan
E-mail : 032d811n@stu.kobe-u.ac.jp

Metallic nanoparticles show the characteristic properties such as nonlinear optical effect and catalytic activity. It is well known that these properties are associated with the excited electron dynamics. Therefore, in order to understand these physical properties of metallic nanoparticles, it is essential to elucidate the excited electron dynamics. In this work, we have carried out the interferometric time-resolved two-photon photoemission study of dodecanethiolate (DT)-passivated Ag nanoparticles supported on the highly oriented pyrolytic graphite (HOPG) substrate in order to directly investigate the excited-electron dynamics of DT-passivated Ag nanoparticles.

Figure 1 shows the two-photon photoemission spectra of HOPG substrate and DT-passivated Ag nanoparticles with mean diameter of 2.9 and 3.6 nm supported on the HOPG substrate, measured with a second harmonic light of Ti:sapphire laser ($\hbar\omega$ ~3.1 eV). These photoemission spectra are plotted as a function of intermediate-state energy in the two-photon photoemission process relative to the Fermi level in Fig. 1. As shown in Fig. 1, two-photon photoemission yields of the present DT-passivated Ag nanoparticles are two or three orders of magnitude higher than that of HOPG substrate. On the other hand, the optical extinction spectra of the present DT-passivated Ag nanoparticles show the broad Mie plasmon resonances centered around 3 eV in photon energy. The excitation energy with photon energy of $\hbar\omega$=3.1 eV resonantly excites the

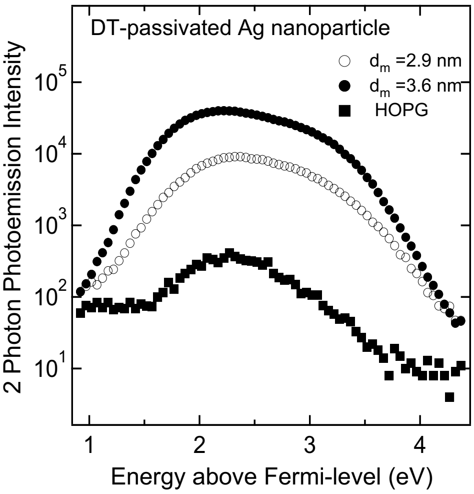

Fig. 1. Two-photon photoemission spectra of DT-passivated Ag nanoparticles with diameter of 2.9 and 3.6 nm supported on the HOPG substrates. Two-photon photoemission spectrum of HOPG substrate is also shown for a comparison.

localized Mie plasmon in DT-passivated Ag nanoparticles. Therefore, this enhancement of two-photon photoemission yield originates from the local field enhancement due to the resonant excitation of Mie plasmon by the exciting laser pulse, and the observed two-photon photoemission spectra are dominated by photoemission intensity from DT-passivated Ag nanoparticles. This indicates that the present two-photon photoemission measurements allow us to selectively investigate the hot-electron dynamics in the Ag nanoparticles.

Interferometric two-pulse correlation measurements of DT-passivated Ag nanoparticles were obtained by monitoring photoemission intensities at a given photoelectron kinetic-energy as a function of the delay time between the pump and probe pulses. From the detailed analyses of the 1ω envelopes, that oscillate at the excitation frequency, and the phase-averaged ones of interferometric two-pulse correrations, we can derive the energy relaxation time of excited electrons. Figure 2 shows the experimental energy relaxation times as a function of excited-electron energy relative to Fermi-level for DT-passivated Ag nanoparticles with mean diameter of 2.9 and 3.6 nm. In general, the dominant process that determines the energy relaxation time of excited-electron on a femtosecond time scale is considered to be electron-electron interaction. Thus, the obtained energy relaxation time reflects the electron-electron interaction. For a comparison, the energy relaxation time due to the electron-electron interaction in bulk Ag previously reported by Aeschlimann *et al.* [1] is also shown in Fig. 2. In the previous report, the energy relaxation time in bulk Ag is quantitatively well reproduced by Fermi-liquid theory. According to Fermi-liquid theory, the energy relaxation time is determined by the density of states in the vicinity of Fermi-level. This means that DT-passivated nanoparticles in the relevant size regime still have a similar electronic structure in the vicinity of Fermi-level and exhibit a similar excited-electron dynamics to bulk Ag. From these results, we will discuss the excited-electron dynamics in the DT-passivated Ag nanoparticles.

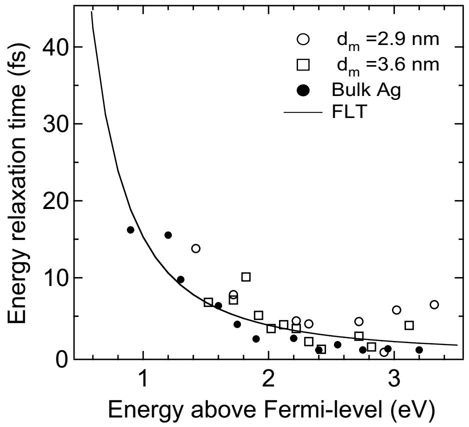

Fig. 2. Energy relaxation times as a function of excited-electron energy relative to Fermi-level for DT-passivated Ag nanoparticles with mean diameter of 2.9 and 3.6 nm, and that of bulk Ag [1]. The solid line shows the calculated ones based on Fermi-liquid theory for bulk Ag.

References

[1] M. Aeshlimann, M. Bauer, and S. Pawlik, Chem. Phys. **205**, 127 (1996).